X-ray and neutron full profile analysis for texture, structure and phase determination of natural samples and more : "Combined analysis approach"

M. Morales, D. Chateigner, L. Lutterotti

Combined analysis approach presentation

- Experimental needs
- Problems on ultrastructures: typical ferroelectric film example
- Methodology-Algorithm
- Ultrastructure implementation
- Results on a case study on typical ferroelectric film
- Residual stresses, Rietveld and texture
- MAUD program implemented codes
- Example showing correlations between stress and texture
- Example showing correlations between anisotropic sizes and texture.

Combined analysis approach illustration through various textured examples: multiphase bulks and thin films

- Geological samples
- $CaCO_3$ mollusc shells
- Biomimetic $CaCO_3$ thin films for medical applications
- Shell fossils: Texture and phylogeny
- Multiphased Cr^{2+}:ZnSe films: combined analysis approach actual limitations

Random powder : $I_{RX\ calc.}(2\theta) = \sum_{hkl,phases} I_{hkl,phases}(2\theta)\, S_{hkl}(2\theta) + bkg(2\theta)$

$$I_{hkl}(2\theta) = A\, S\, |F_{hkl}|^2\, m_{hkl}\, \frac{L_p}{V_c^{\,2}}$$

- A → absorption
- S → scale factor (phase abundance)
- $|F_{hkl}|^2$ → structure factor (includes Debye-Waller term)
- m_{hkl} → multiplicity
- L_p → Lorentz- polarisation factor
- V_c → unit-cell volume

$$S_{hkl}(2\theta) = S^{I}_{hkl}(2\theta) * S^{S}_{hkl}(2\theta)$$

- $S_{hkl}(2\theta)$ → Peak profile function
- $S^{I}_{hkl}(2\theta)$ → instrumental broadening ➔ powder standard calibration
- $S^{S}_{hkl}(2\theta)$ → Sample aberrations = crystallite sizes (isotropic or anisotropic) + rms microstrains $\varepsilon^* = <\varepsilon>^2$ due to linear and point defects, stacking faults…

Texture :

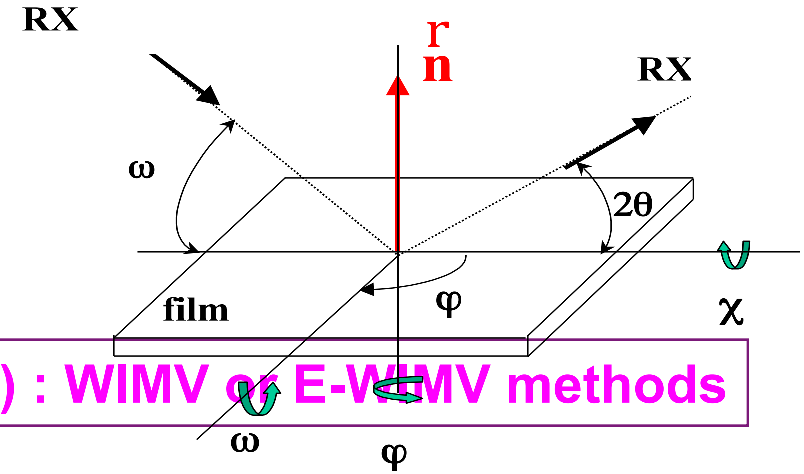

Correction of intensities for texture :

$$I_{hkl}(2\theta, \chi, \varphi) = I_{hkl}(2\theta)\, P_{hkl}(\chi, \varphi)$$

Orientation Distribution Function (ODF) : WIMV or E-WIMV methods

From spectra : pole figures $P_{hkl}(\chi, \varphi)$

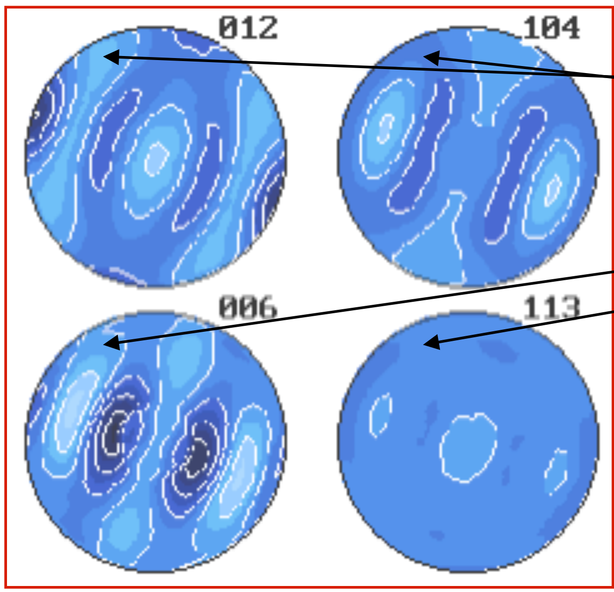

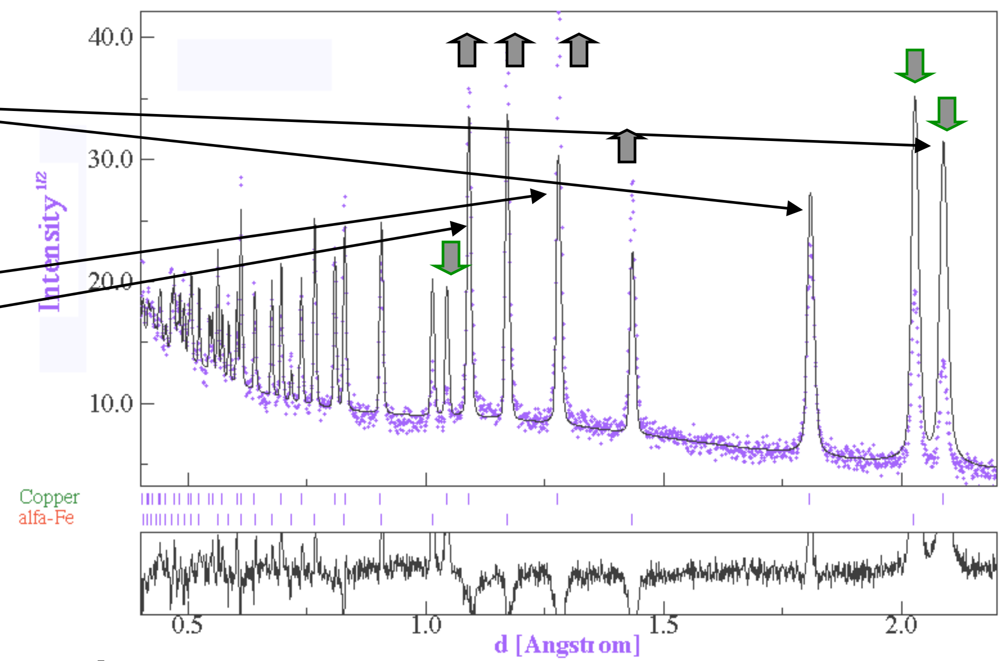

ODF = statistical distribution of orientations

Combined analysis approach

Minimum experimental requirements:

1D or 2D Detector + 4-circle diffractometer (X-rays and neutrons)

CRISMAT, ILL

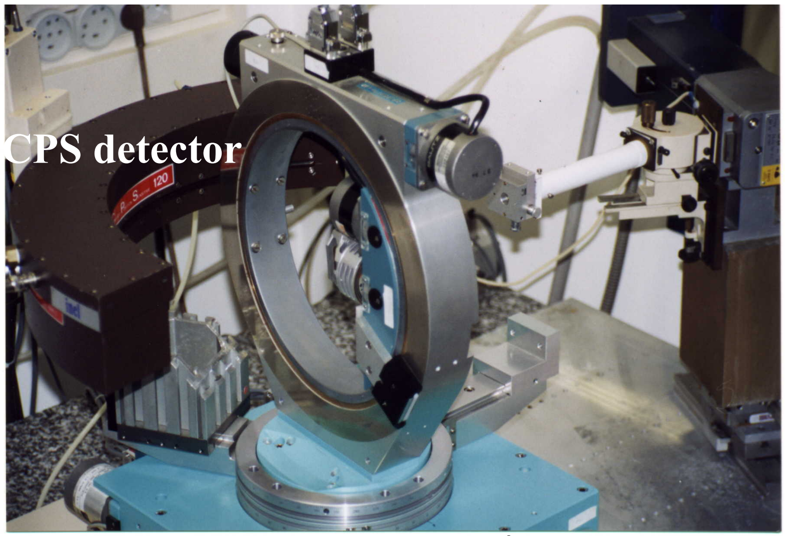

$\lambda_{Cu\ \alpha}$ = 1.5418 Å

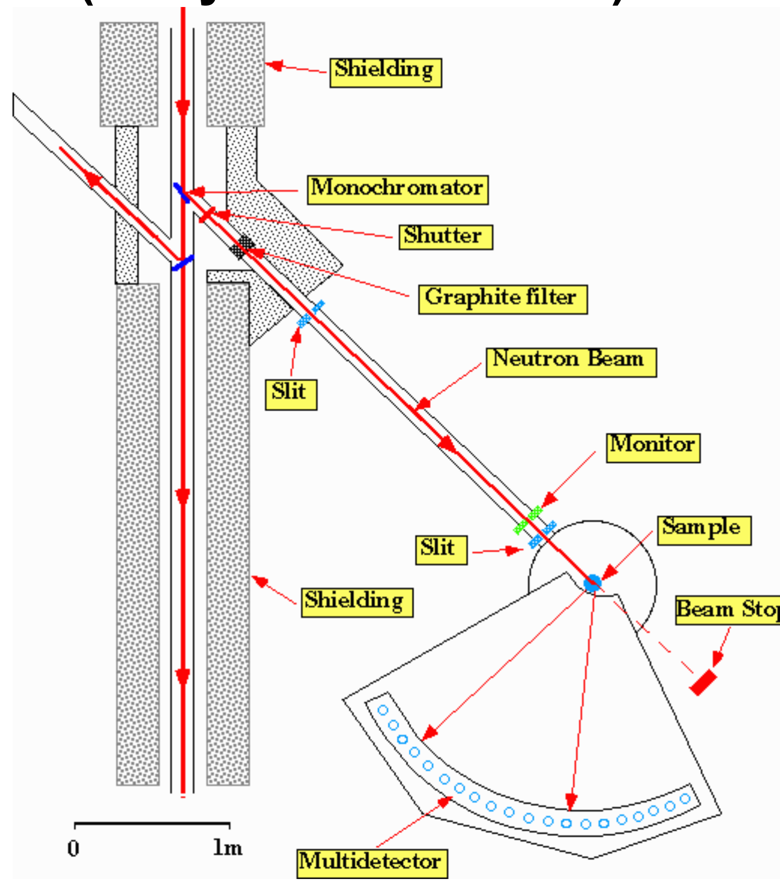

$\lambda_{neutron}$ = 2.533 Å

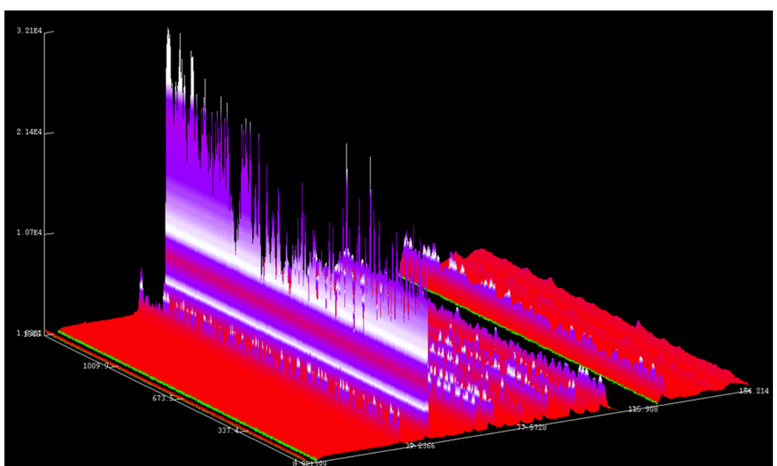

~1000 experiments (2θ diagrams) in as many sample orientations

Combined analysis approach

Instrument calibration :

instrumental resolution function

↓

mapping spectrometer space with :

- **KCl or LaB_6 powder standards for X-rays**
- **Belemnite rostrum having large calcite grains for neutrons**

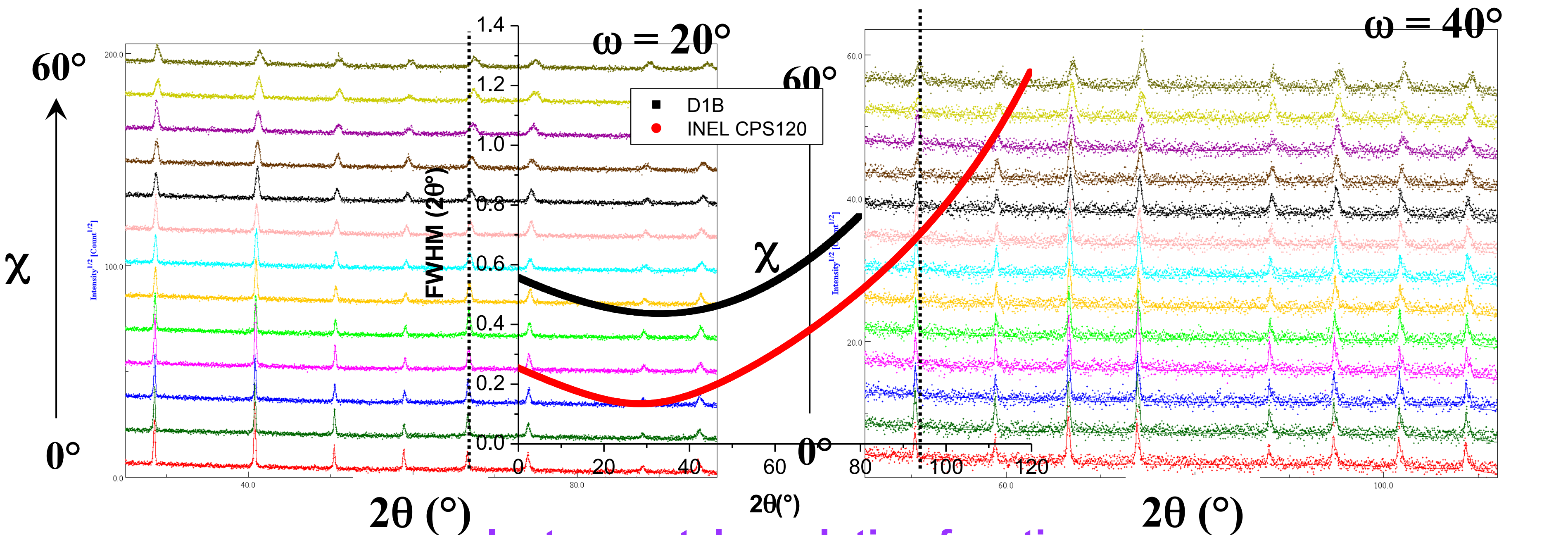

Instrumental resolution functions

peaks widths and shapes FWHM (ω, χ, 2θ …), misalignments, defocusing (2θ shift, Gaussianity, asymmetry) …

Problems on ultrastructures : example of $Pb_{0.76}Ca_{0.24}TiO_3$ (PTC) ferroelectric films

Ferroelectric properties optimisation: polarisation vector along $\vec{c}$ i.e. <001> // $\vec{n}_{film}$

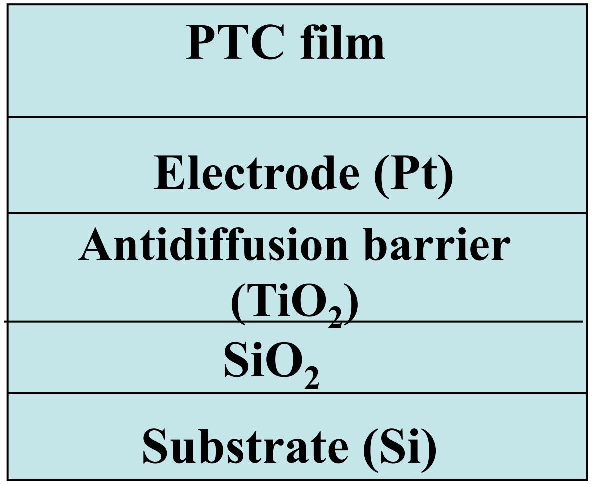

Pseudo cubic phase of PTC

Sum X-ray diagram (χ, φ)

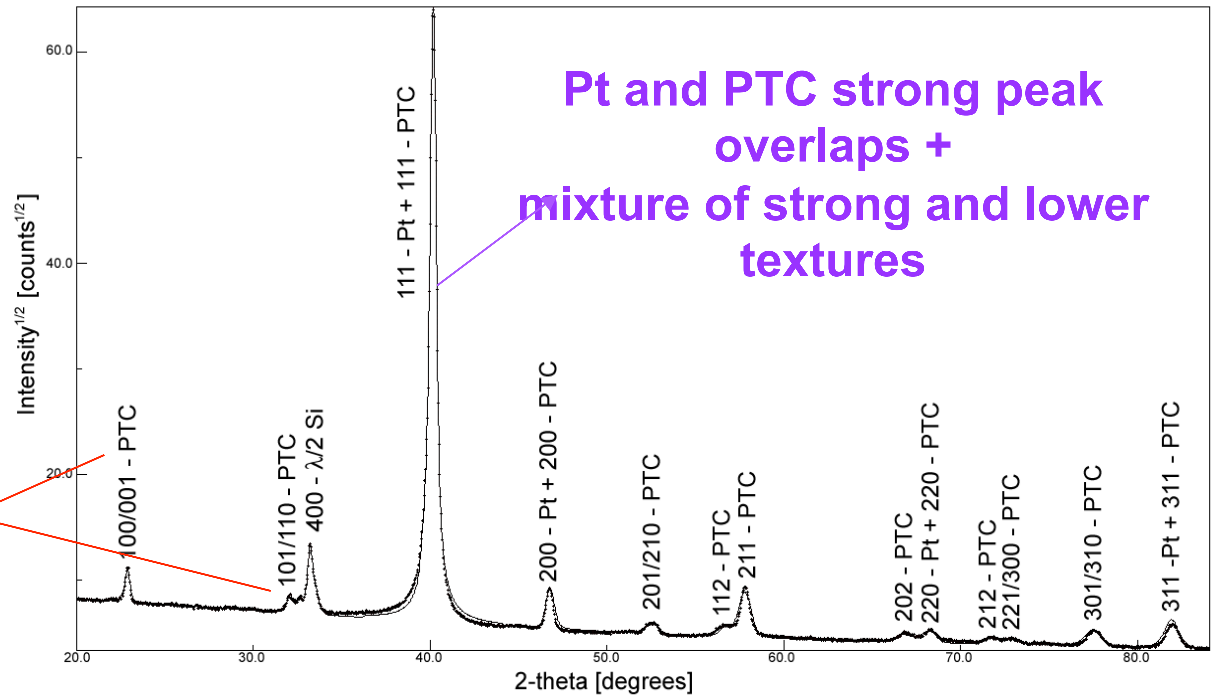

♦ texture effect not fully removable : structure and microstructure

♦ structure and microstructure unknown : texture

combined analysis approach necessary !!!

X-ray combined analysis approach

Algorithm and methodology

Intensity corrections for textured samples:

$$I_{hkl}(2\theta, \chi, \varphi) = I_{hkl}(2\theta)\, P_{hkl}(\chi, \varphi)$$

MAUD program (Material Analysis Using Diffraction) :
(Marquardt non linear least squares fit, for instance)

Rietveld cycle :
Structure, microstructure

QTA cycle :
WIMV or E-WIMV
Orientation distribution function

1st cycle: integrated intensities (Le Bail extraction) ➔
Pole figure construction $P_{hkl}(\chi,\varphi)$.

Ultrastructure PTC/Pt implementation

Corrections are needed for volumic/absorption changes when the samples are rotated.

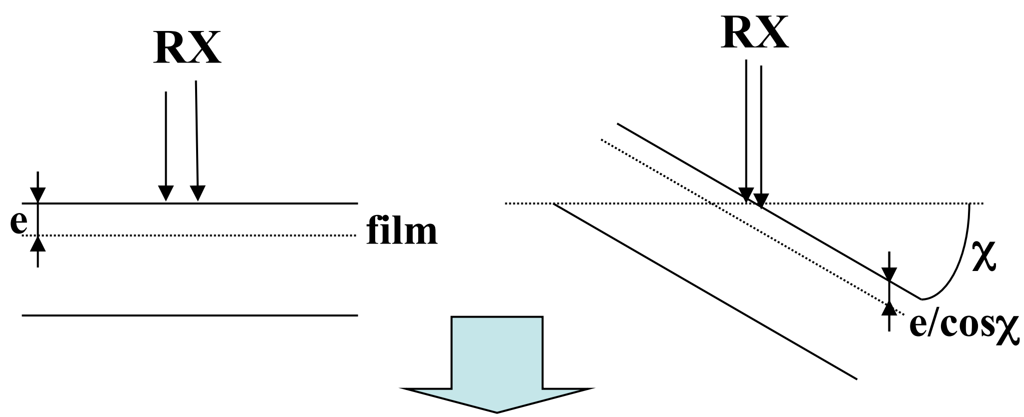

with a CPS detector :

$$\underline{\text{PTC}} : C_\chi^{\text{top film}} = g_1 (1 - \exp(-\mu T g_2 / \cos\chi))/(1-\exp(-2\mu T / \sin\omega\cos\chi))$$

$$\underline{\text{Pt}} : C_\chi^{\text{cov layer}} = C_\chi^{\text{top film}} (\exp(-g_2 \sum \mu'_i T'_i / \cos\chi))/(\exp(-2 \sum \mu' iT'_i / \sin\omega\cos\chi))$$

Gives access to individual thicknesses in the refinement

$Pb_{0.76}Ca_{0.24}TiO_3$ (PTC) film

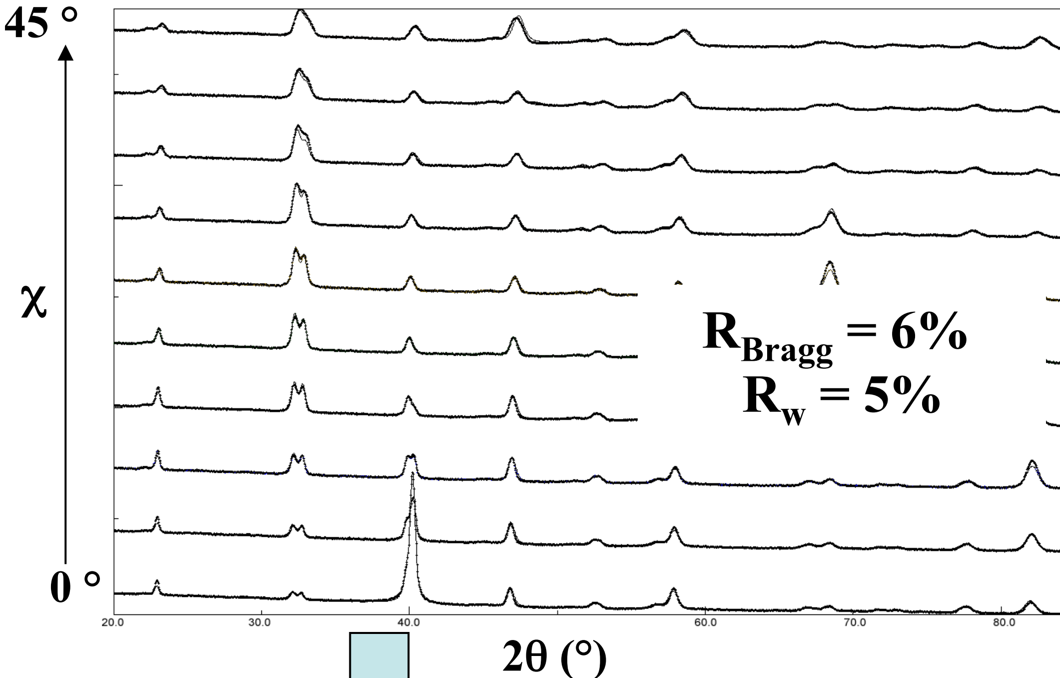

Pt

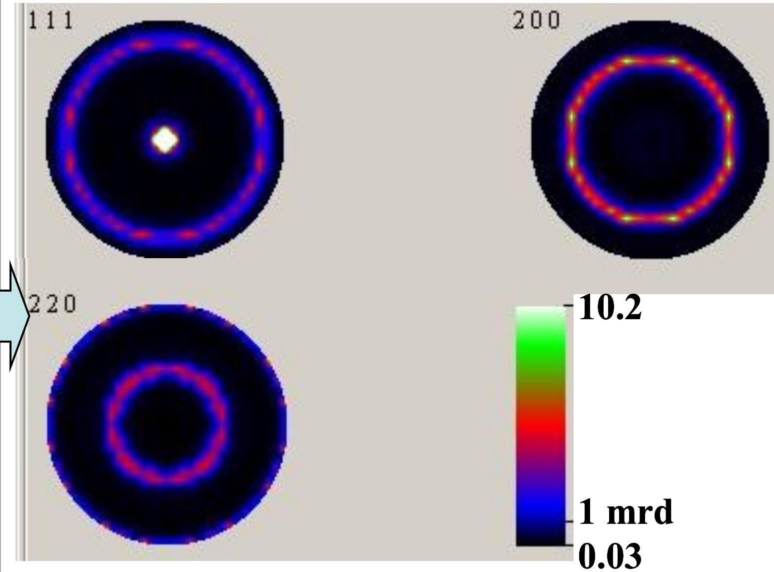

a = 3.955(1) Å, T' = 462(4) Å
t'_{iso} = 458(3) Å, ε' = 0.0032(1)

PTC

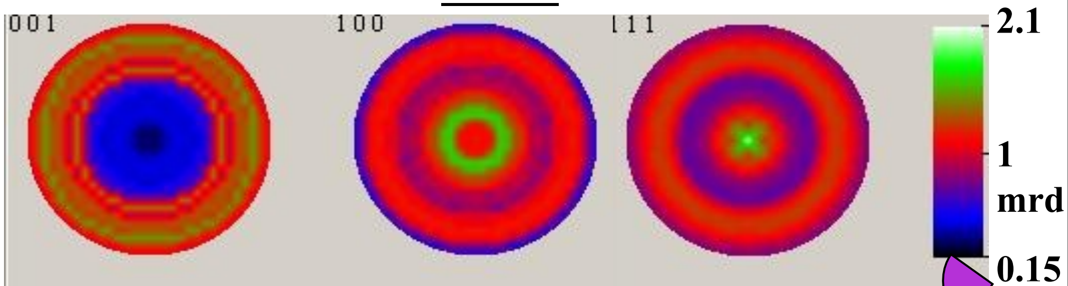

a = 3.945(1) Å, c = 4.080(1) Å
T = 4080(10) Å, t_{iso} = 390(7) Å
ε = 0.0067(1)

15% of $\vec{c}$ axes non oriented in film plane → some weak polarization properties

Ricote, Morales et al. TSF 450, (2004) 128.

Residual stresses, Rietveld and texture

♦ peak **shifts** bias **structure** and **texture** determination → **residual stress** must be determined

♦ **different deformation** of differently oriented crystallites → **texture** influences **residual stress**

combined analysis approach necessary !!!

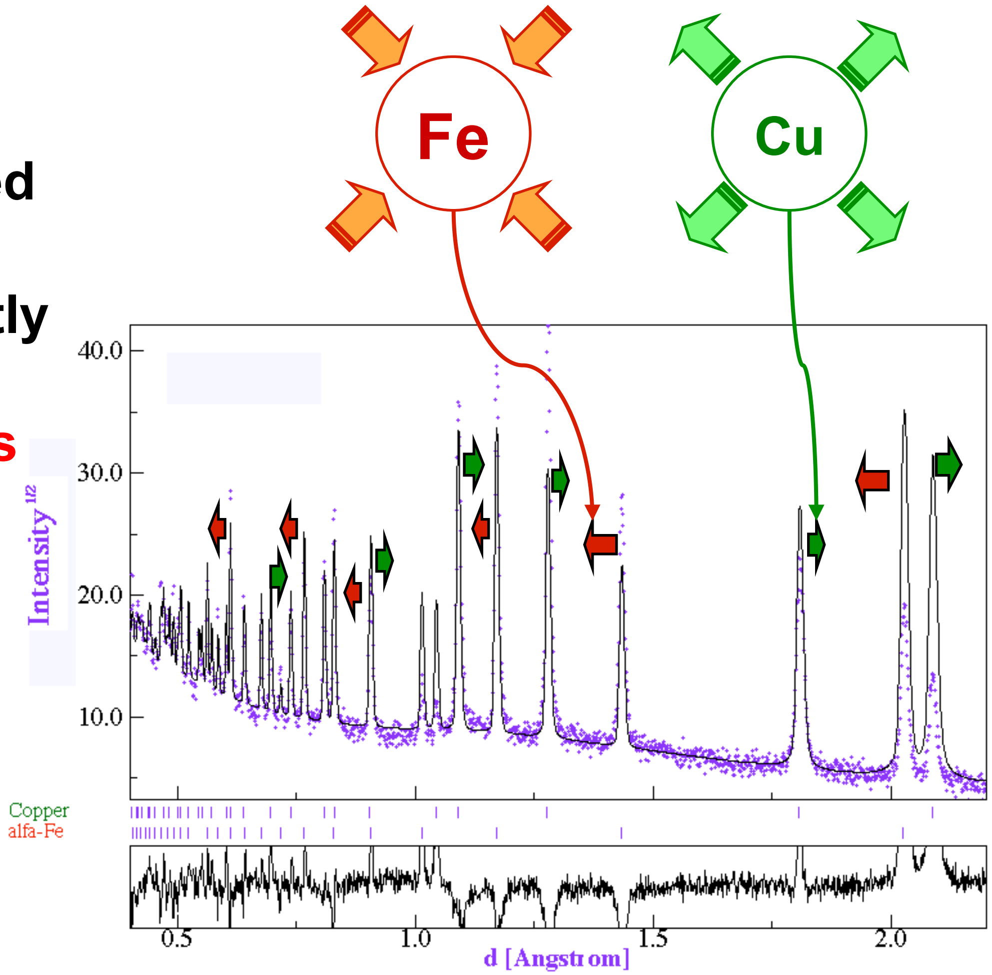

Non-linearity in sin$^2\psi$ relation observed due to stress gradients or texture → Reuss, Voigt, Hill, **Bulk geometric mean approaches.**

MAUD implemented codes :
parameter interdependency + formalism

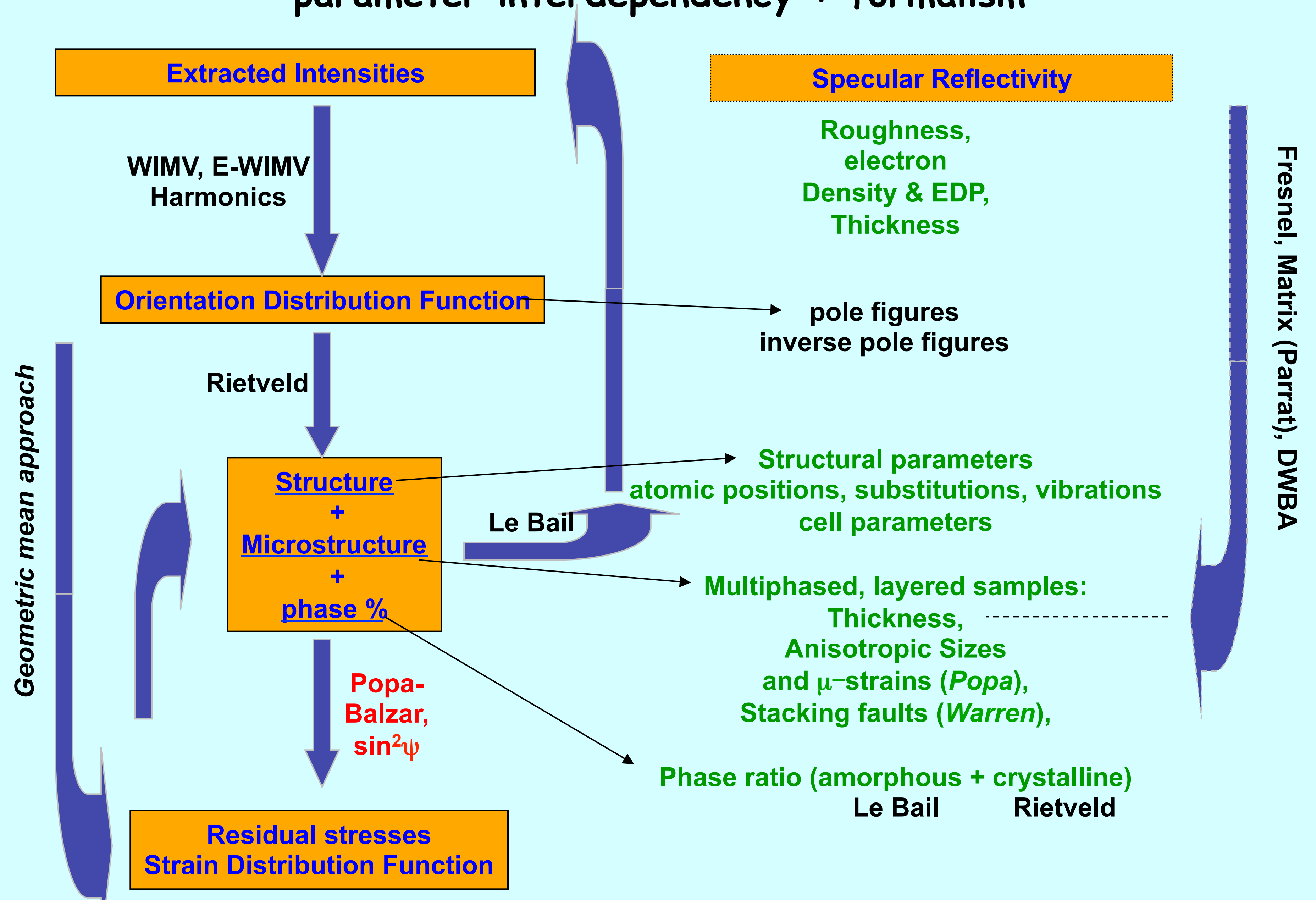

Combined analysis approach

Combined analysis approach on PTC films :

Substrate influence on residual stress and texture

Tensile stress

PTC on $Pt/TiO_2/(100)Si$

PTC on Pt/(100)MgO

PTC on $Pt/(100)SrTiO_3$

Compressive stress

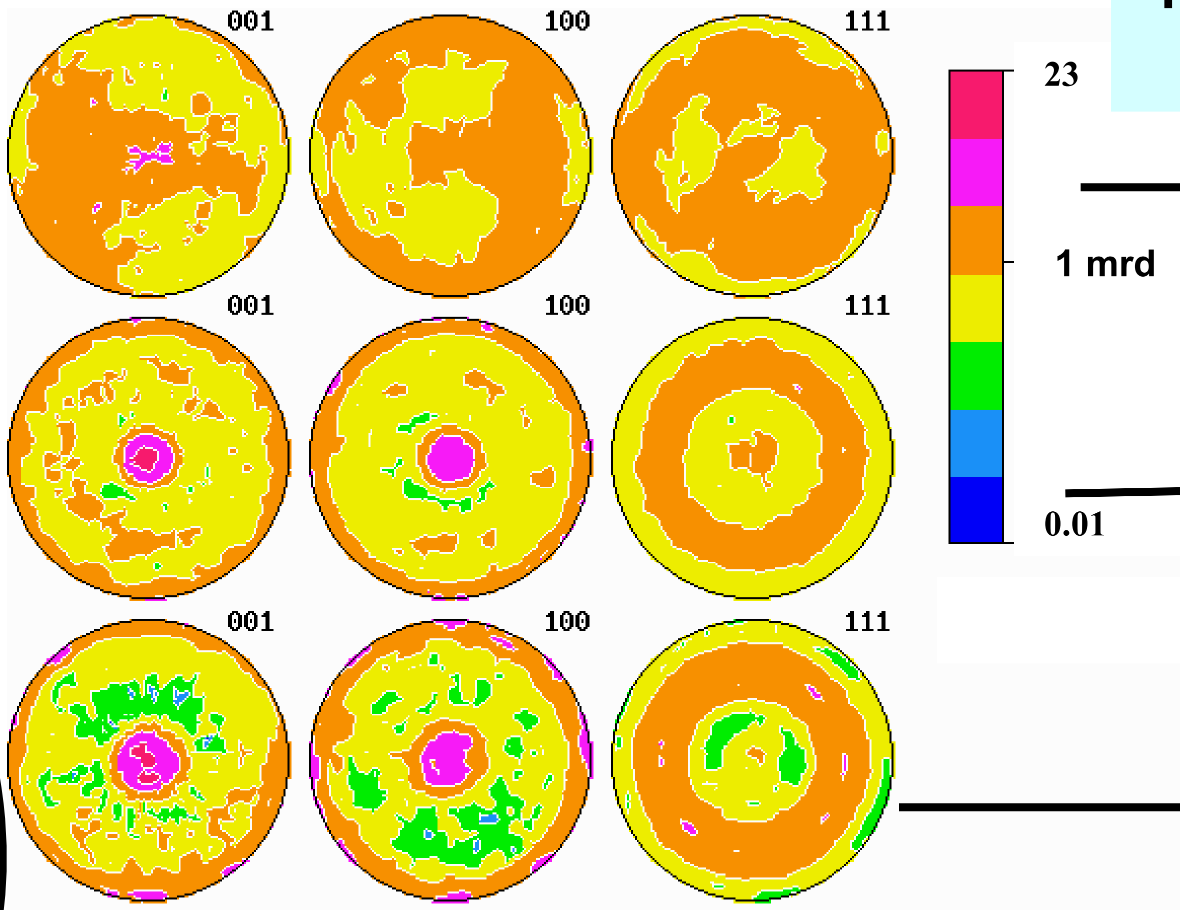

Texture Index (m.r.d.²)

2.1

5.1

7.9

Enhancement of <001> texture

Anisotropic sizes and texture: nanocrystallized Si thin film example

Morales et al. JAP 97 (2004) 034307.

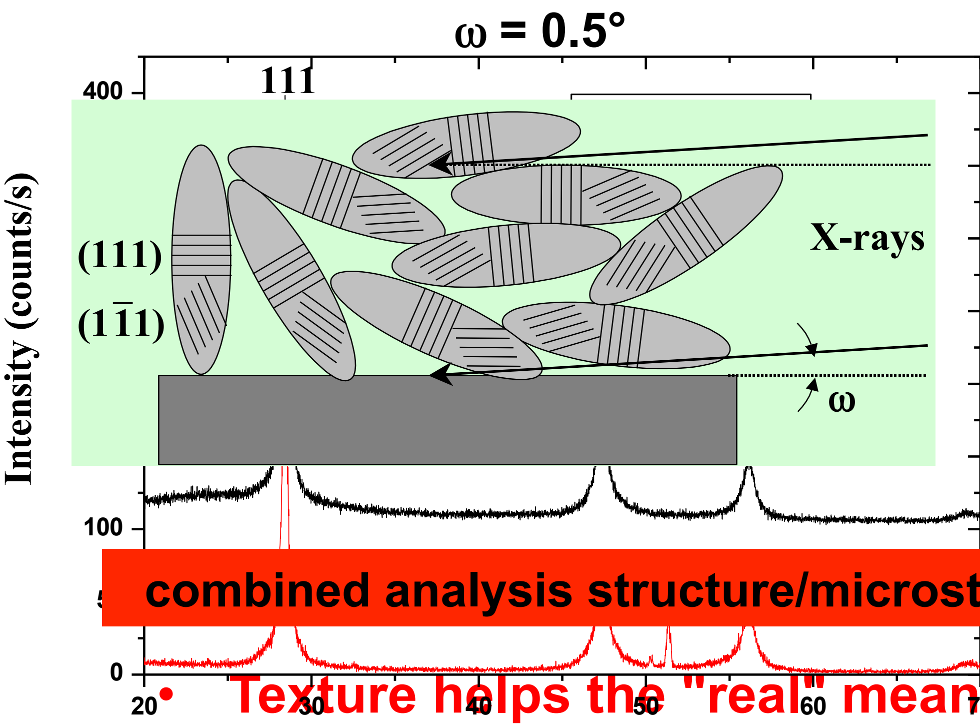

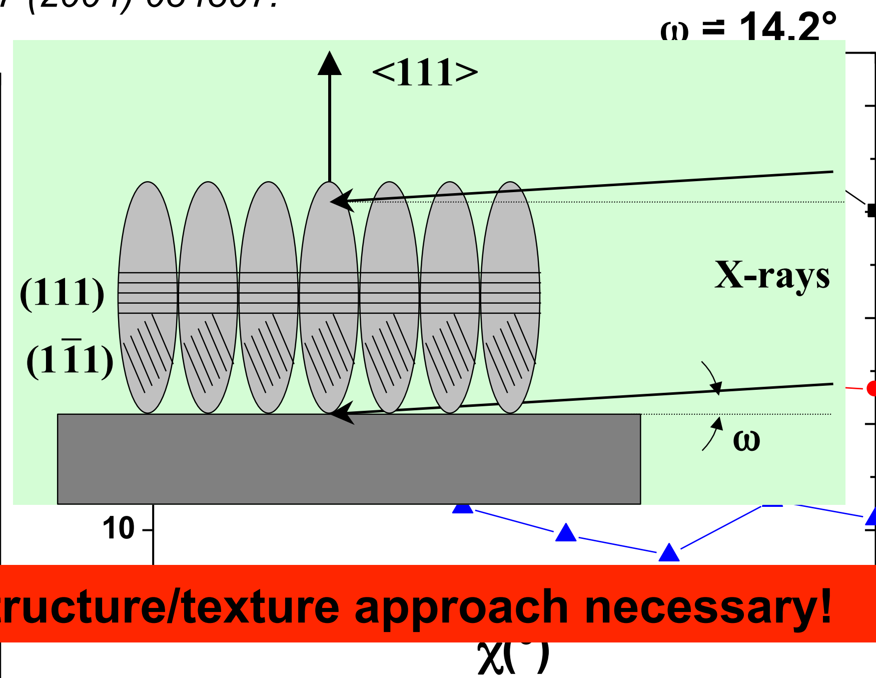

combined analysis structure/microstructure/texture approach necessary!

- Texture helps the "real" mean shape determination
- Determination by peak deconvolution + Popa formalism →

Film: fiber texture with multiple orientations →
QTA analysis necessary !

Anisotropic crystallite shape :
Popa formalism

$$<R_{\mathbf{h}}> = R_0 + R_1P_2^0(x) + R_2P_2^1(x)\cos\varphi + R_3P_2^1(x)\sin\varphi + R_4P_2^2(x)\cos2\varphi + R_5P_2^2(x)\sin2\varphi + \ldots$$

$$<\varepsilon_{\mathbf{h}}^2>E_{\mathbf{h}}^4 = E_1h^4 + E_2k^4 + E_3\ell^4 + 2E_4h^2k^2 + 2E_5\ell^2k^2 + 2E_6h^2\ell^2 + 4E_7h^3k + 4E_8h^3\ell + 4E_9k^3h + 4E_{10}k^3\ell + 4E_{11}\ell^3h + 4E_{12}\ell^3k + 4E_{13}h^2k\ell + 4E_{14}k^2h\ell + 4E_{15}\ell^2kh$$

→ microstrain

Combined analysis approach : nc –Si films

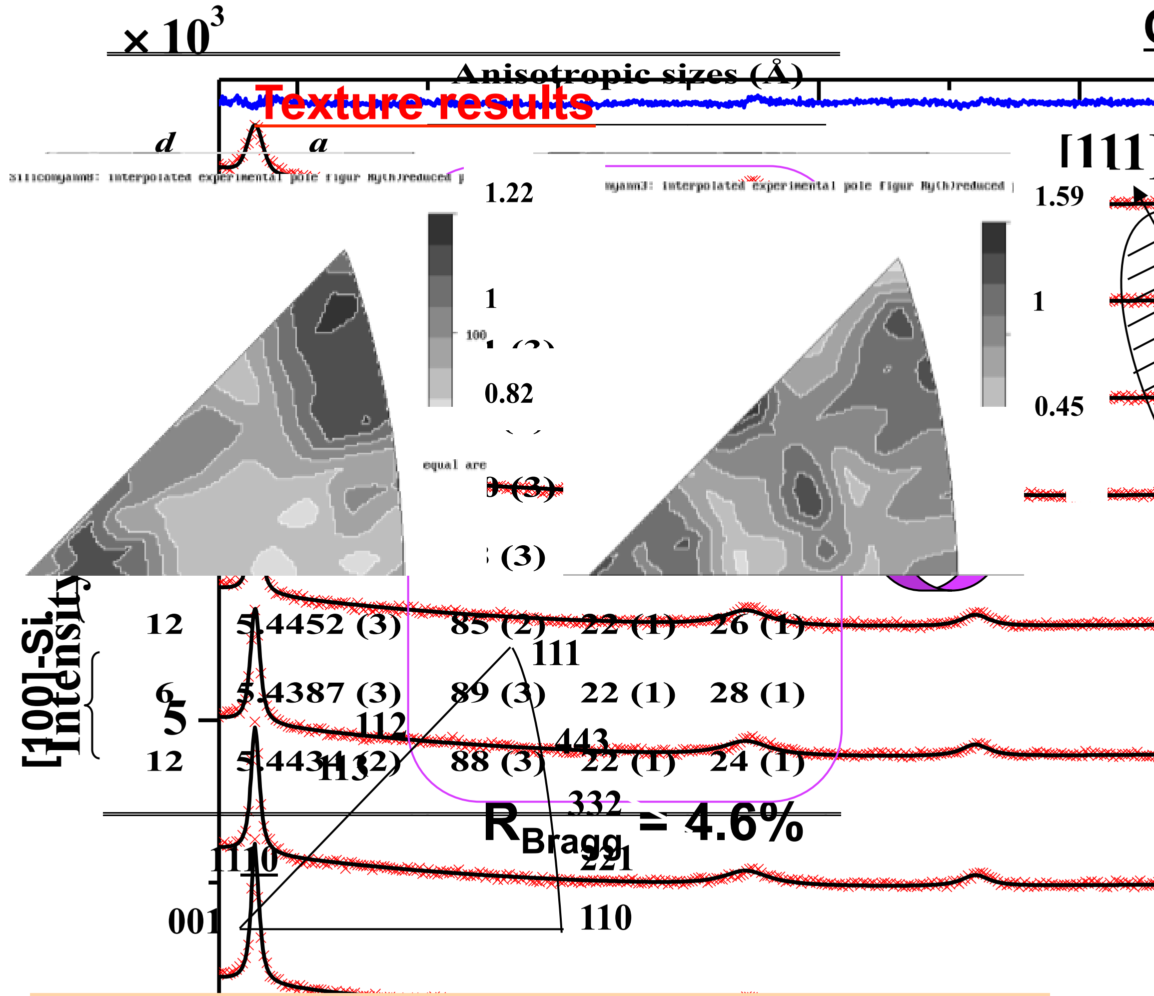

Crystallite shape schematic representation:

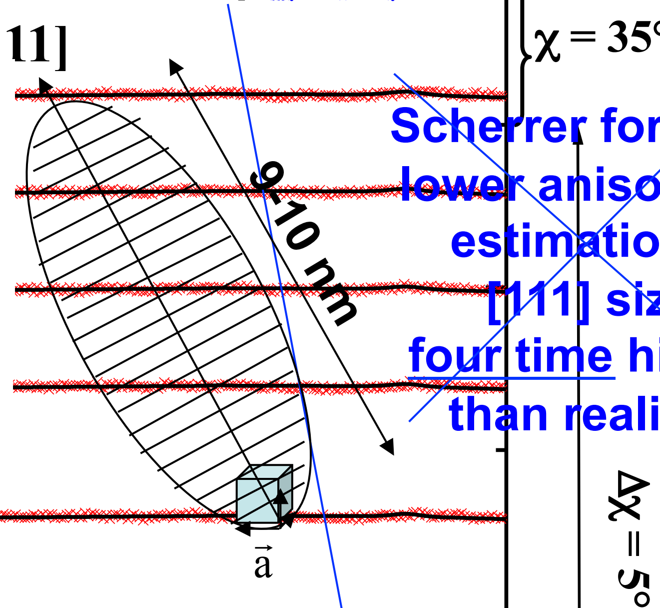

Scherrer formula: lower anisotropy estimation + [111] size four time higher than reality !

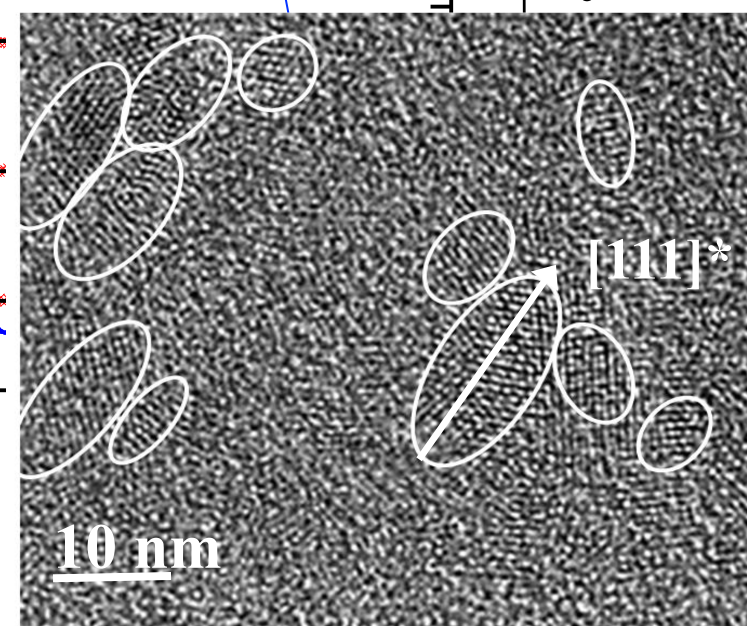

fibre texture with multiple orientations never reaching pure <111> texture component whereas [111] elongated crystallite → in agreement with HRTEM observations

↳ Illustration of the combined analysis approach

QTA = important tool in geology to describe anisotropy of fabrics, the mollusc and fossils phylogeny and geophysics.

1) Metamorphic Amphibolites from Alps:

(M. Zucali, G. Gosso, DES, Milano)

↳ X-ray and neutron diffractions applied to QTA analysis of naturally deformed glaucophanite from the Western Italian Alps

= winchitic amphiboles (≥ 97%)

↓

Comparison of two techniques reveals limits and problems of texture analysis related to strongly deformed polymineralic samples.

↳ ODF measured and computed with 3 methods :

- Direct X-ray peak integrations
- X-ray combined analysis
- Neutron combined analysis

(χ, φ) summed X-ray diagrams

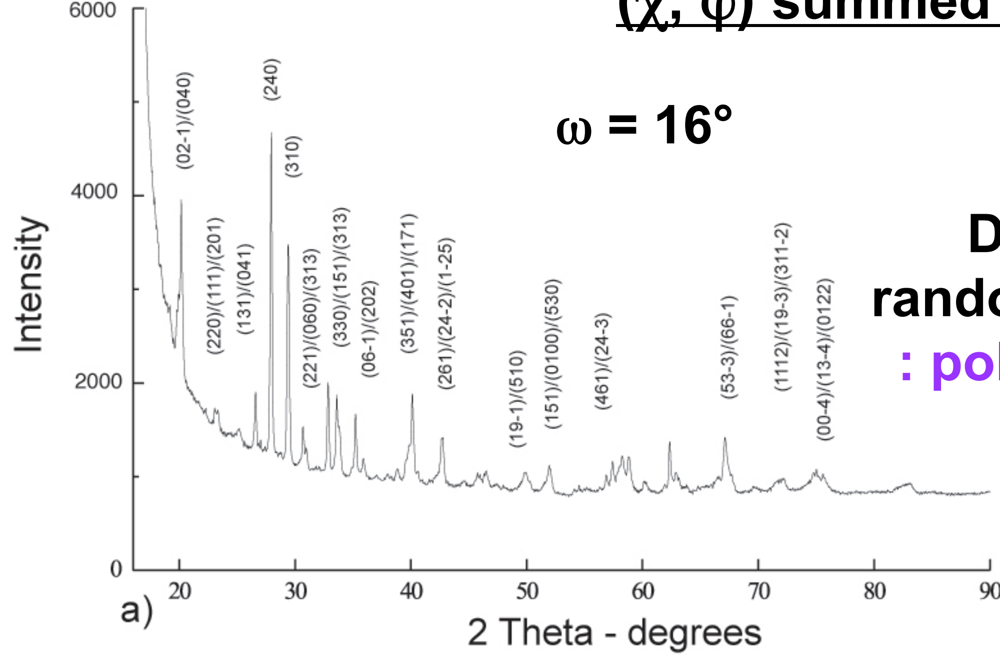

Diagrams approximately close to random powder due to defocusing effect : pole figures incompletely measured !

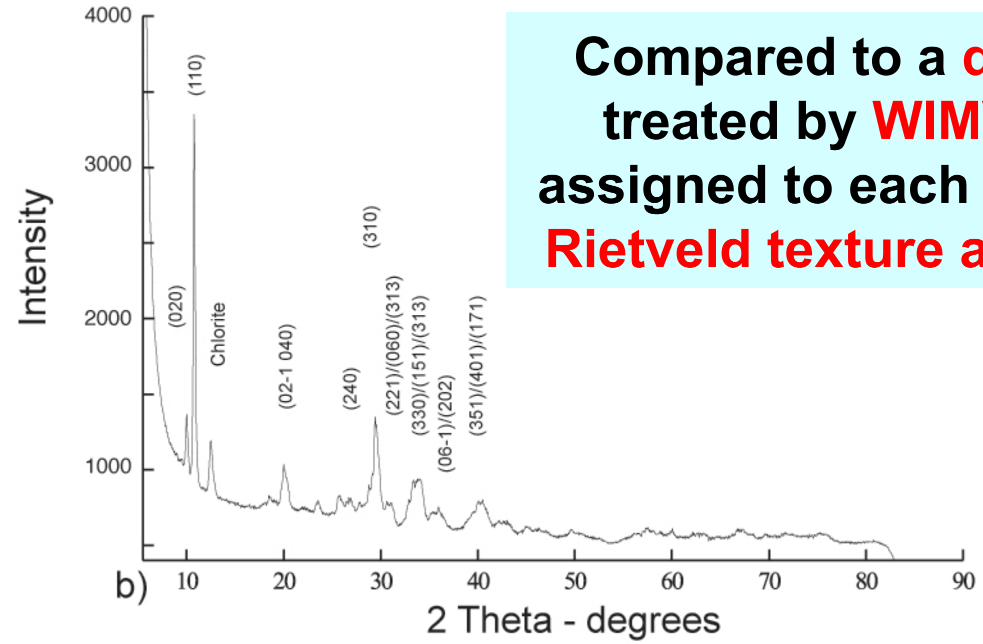

Compared to a direct integration + some overlaps treated by WIMV method (intensity contribution assigned to each component of the muti-pole figure) Rietveld texture analysis is better to solve overlaps!

Neutron diagrams (D1B, ILL)

Summed diagram close to a random powder (no defocusing effect) even if blind areas remain !

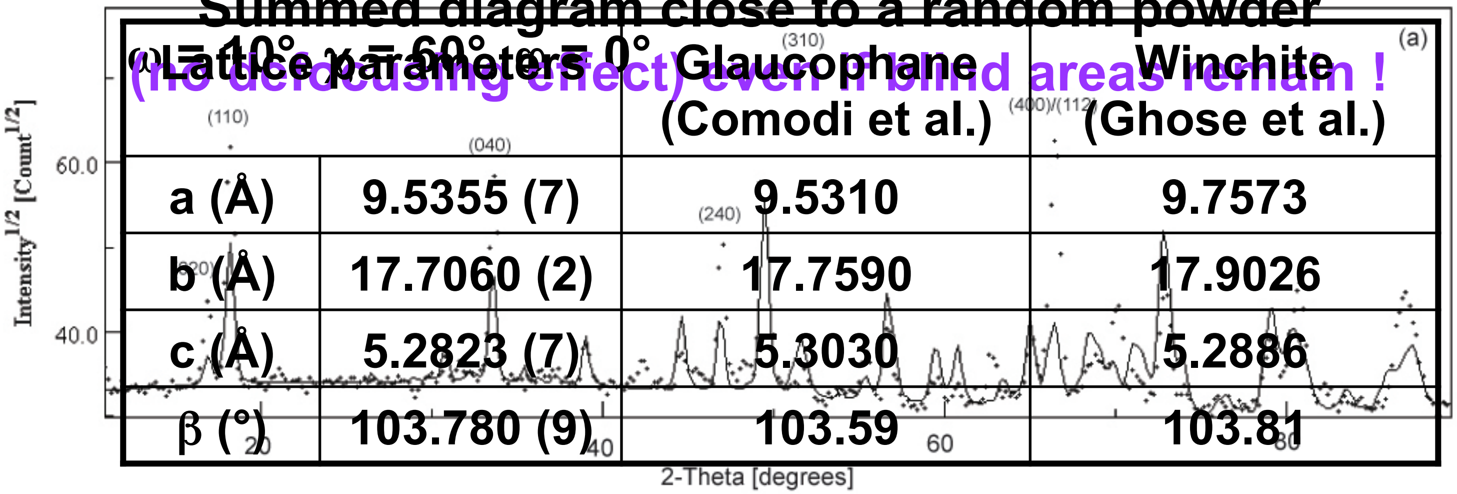

Lattice parameters		Glaucophane (Comodi et al.)	Winchite (Ghose et al.)
a (Å)	9.5355 (7)	9.5310	9.7573
b (Å)	17.7060 (2)	17.7590	17.9026
c (Å)	5.2823 (7)	5.3030	5.2886
β (°)	103.780 (9)	103.59	103.81

Few overlaps in comparison with X-rays !

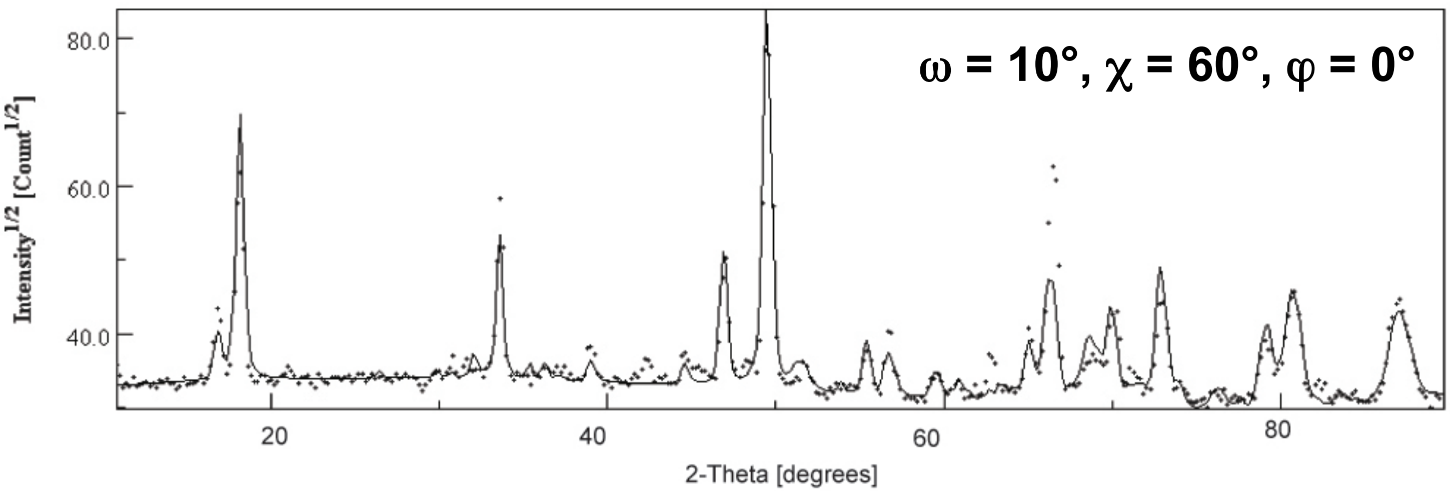

Texture correction : neutron combined analysis approach with only one phase present (amphibole)

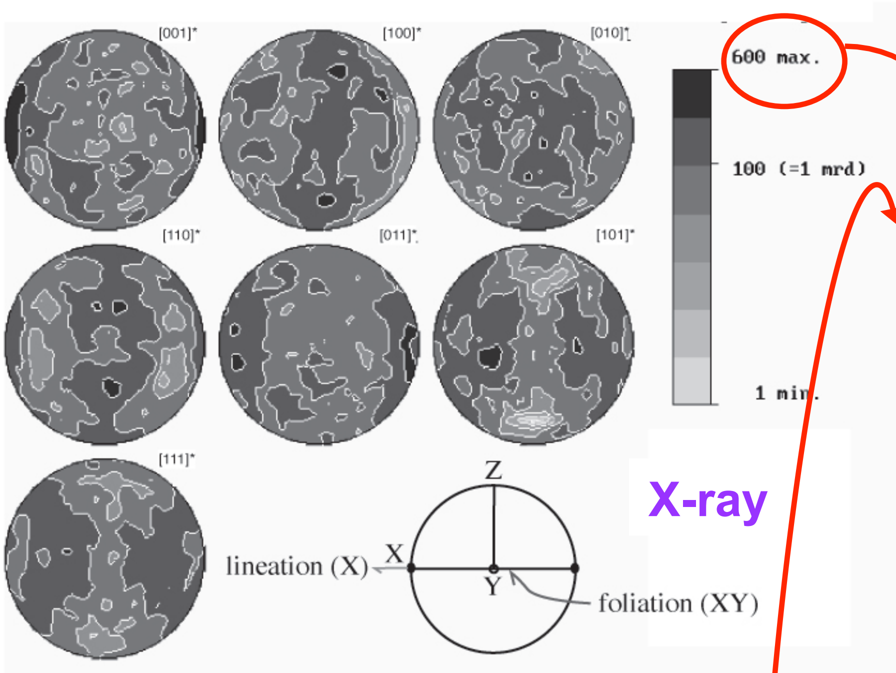

Grain size problems + heterogeneity of individual amphibole minerals → Neutron radiation better to probe the whole rock !!
(more penetrative + large volume sample tested → better statistic)

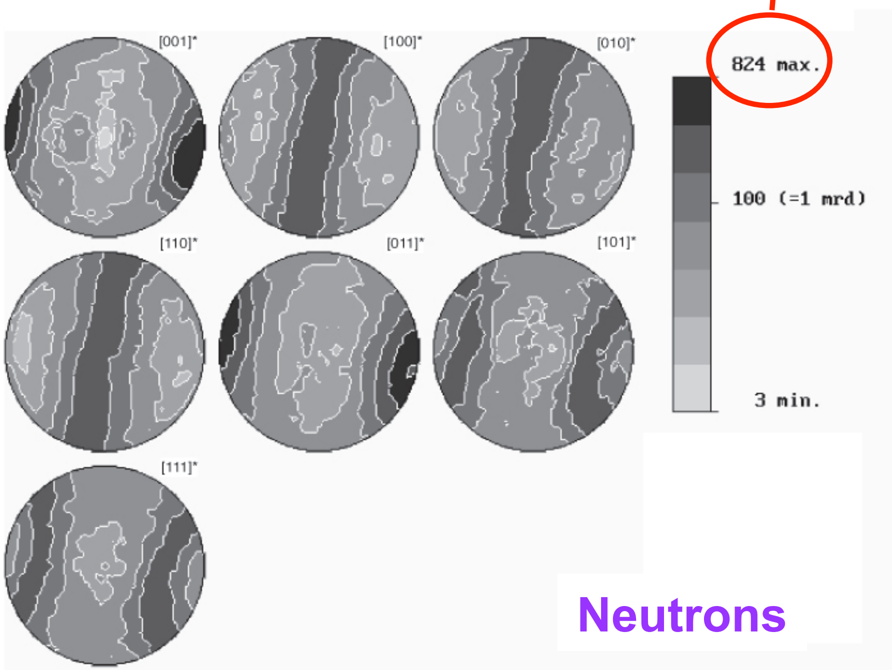

Texture comparable with those described in amphiboles deformed at ≠ pressure and temperature: [001]* and [110]* directions mainly // and ⊥ to lineation

Texture of amphiboles collected at ≠ places and in ≠ lithologic types

↳ **White mica** and chlorite partially **replace amphibole** or fill small fractures with quartz and carbonates

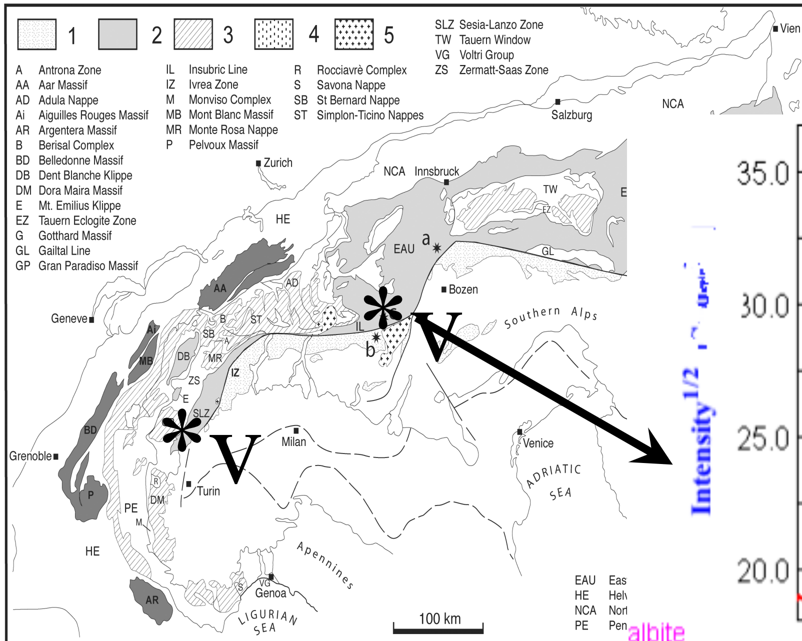

Fig. 1* –Tectonic sketch map of the Alpine chain: shaded areas correspond to continental Alpine crust. Legend: 1 = Southalpine basement; 2 = Austr 4 = Helvetic basement; 5=Tertiary intrusive stocks. Stars localise the Texel Gruppe metapelites in the Oetztal nappe (a), the Eastern Orobic Alps met (b) and the Mortirolo Pass area in Central Austroalpine domain of the Languard-Campo Nappe (c).

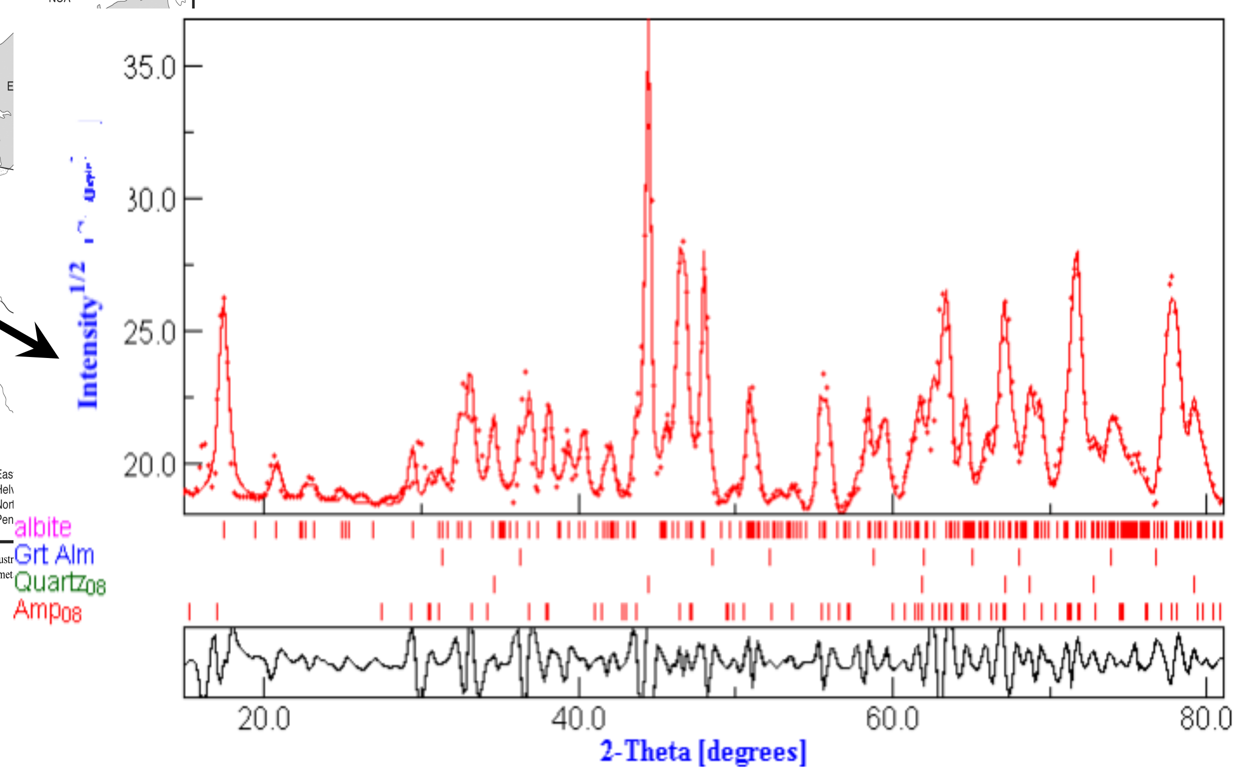

Combined approach allows to access to pole figures for most of the rock-forming minerals (even for mica)

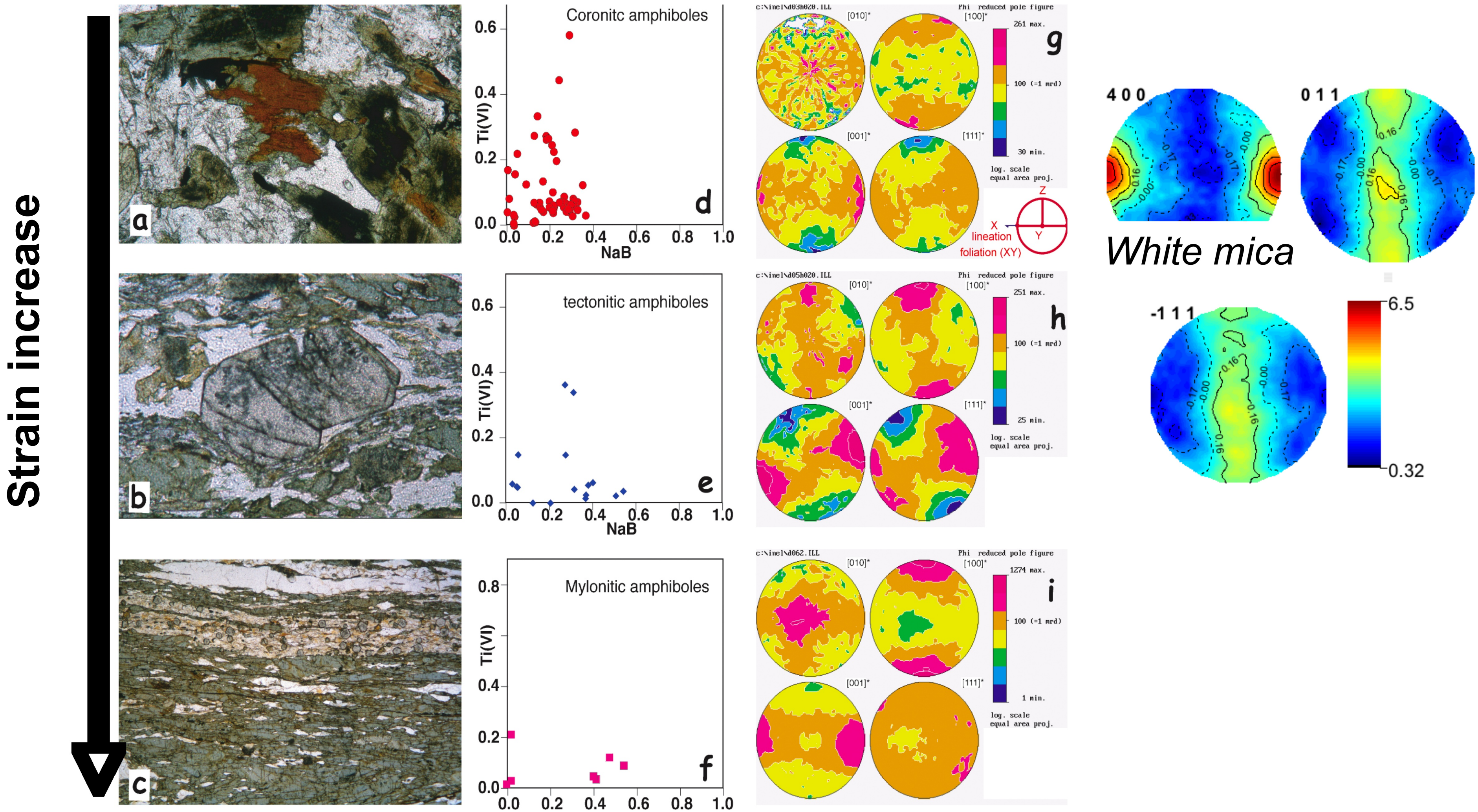

Degree of fabric evolution due to:
- deformation partitioning at metric-scale
- degree of chemical changes within amphiboles
- evolving metamorphic conditions during Alpine subduction (60-100 Million years).

↳ Illustration of the neutron combined analysis approach

2) Polyphased Mylonite : Palm Canyon, CA

(H.-R. Wenk, DEPS, Berkeley; B. Ouladdiaf ILL, Grenoble)

↳ crystallite orientations strong incidence on deformations occurring during geological processes + mutual deformations of several phases may play important rules in the global phenomena.

↳ rock sample from Palm Canyon = low symmetry polyphase materials deformed in the Santa Rosa mylonite zone during the late Cretaceous.

↳ Texture resolved with neutrons (D1B, ILL) for polyphase rock (quartz, biotite and plagioclase considered as pure albite).

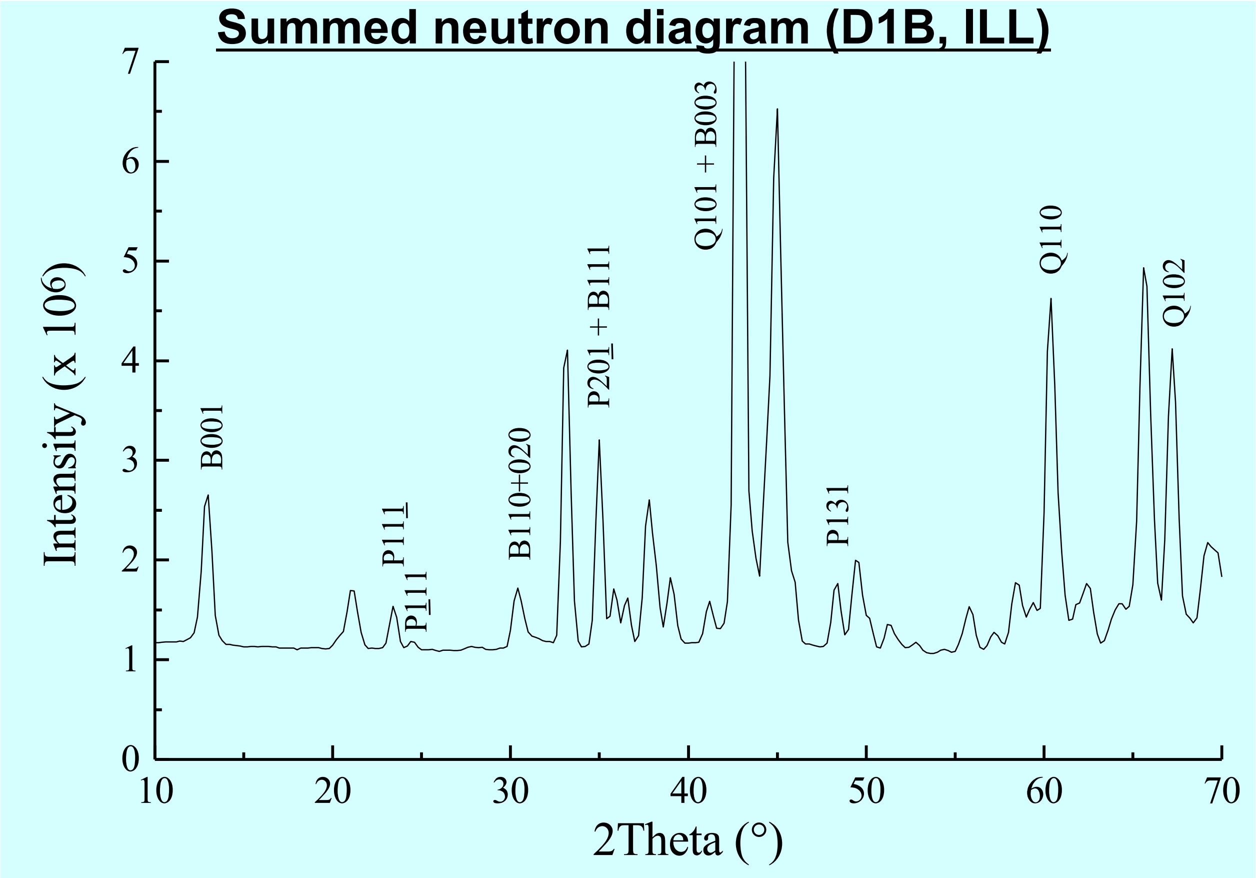

Strongly overlapped peaks intra- and inter-phases + textured sample → Combined analysis approach

Only 3 phases considered

PC 82 mylonite	Biotite	Quartz	Albite	Anorthite	K-spar
Composition (weight %)	9.0	24.2	31.7	17.4	14.1
Space group	C2/m	R3	C-1		

Biotite:
010 axes // lineation direction

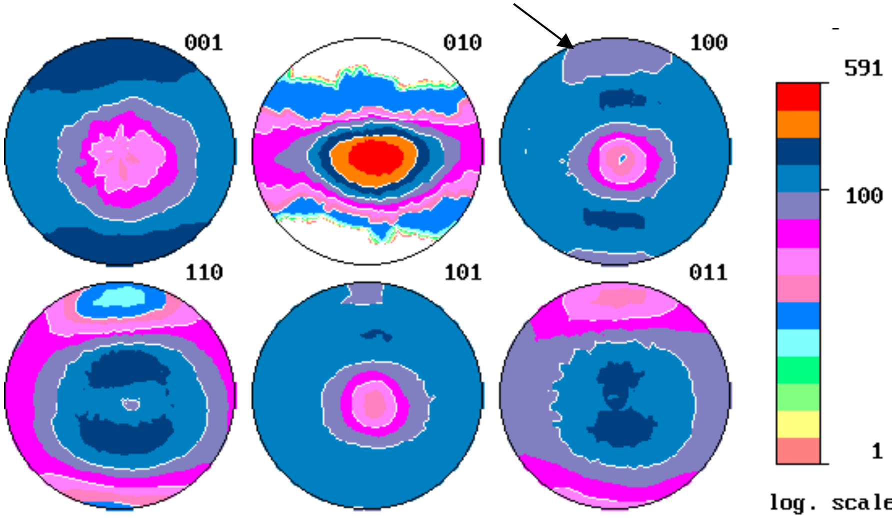

Quartz:
Max. ODF with c-axes in the foliation plane + a-axes // lineation direction

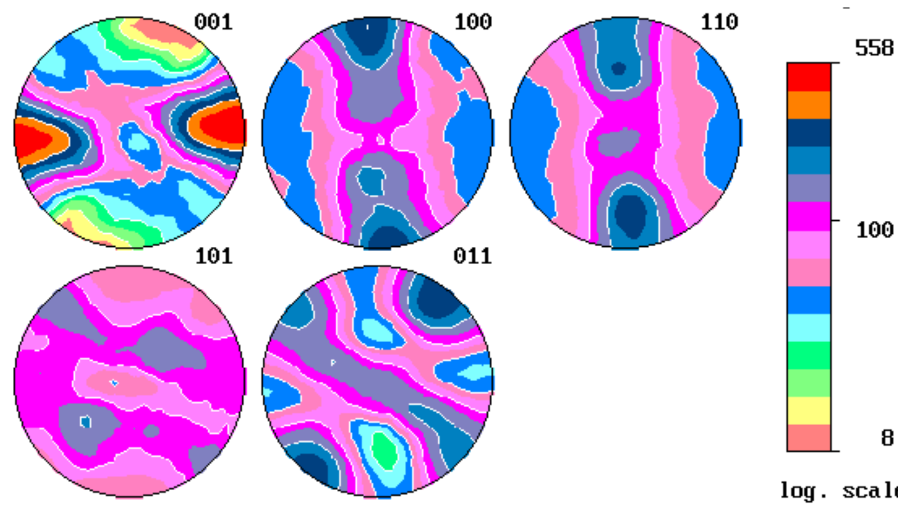

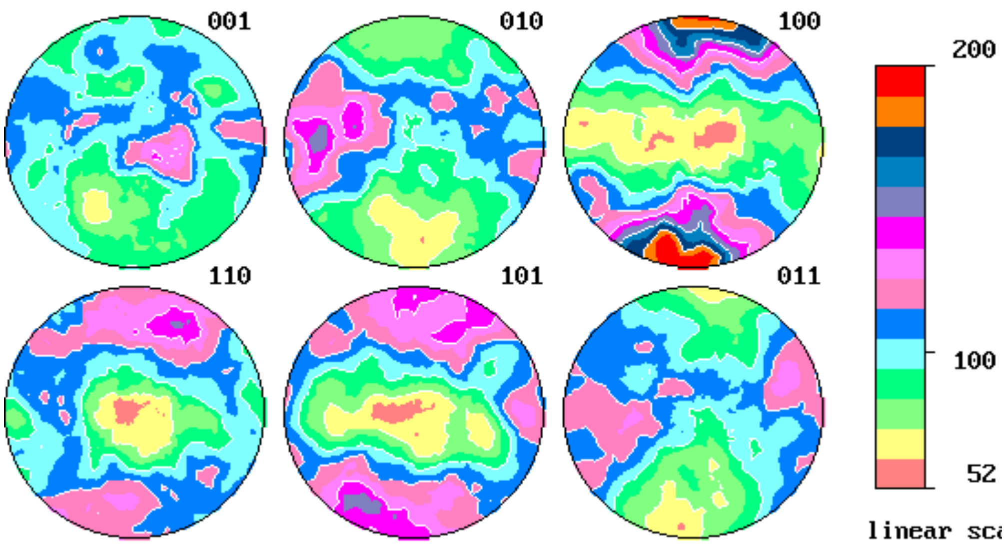

Albite:
a-axes // lineation + b- and c-axes randomly distributed around a-axes.

Orientationnal relationships

// Lineation:

<100>*-quartz // <100>*-albite // <010>*-biotite

// foliation:

<001>*-quartz // <100>*-biotite

Geological samples

↳ Illustration of the X-ray combined analysis approach

3) Texture and structure of mollusc shells:
Charonia lampas lampas and Pinctada maxima
(S. Ouhénia Thesis – december 2008)

↳ Tremendous work on mollusc shell growth + mollusc shell = fascinating examples of high resistant biocomposite materials.

Mollusc shell = two polymorphs of $CaCO_3$: aragonite + calcite + organic phases

For example: the organic part of the red Abalone *Haliotis rufescens* shell represents around 1 to 5% of the total weight and shell is 3000 time more resistant than pure geological aragonite!

↳ Nacre (aragonite) is significant in medicine (orthopedics) due to high osteoinductive properties. Maya Indians of Honduras already used nacre for dental implants 2000 years ago!

↳ In modern orthopedic medicine, aragonite of Pinctada maxima stimulates bone growth by human osteoblasts.

a) *Charonia lampas lampas*: Aragonitic shell

Mediterranean sea and Eastern Atlantic carnivorous gastropod mollusc. Protected species in mediterranea.

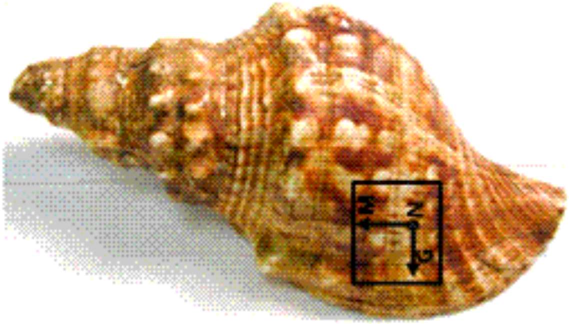

N = normal , M = margin and G = growth directions

Microstructure never reported → determination by using SEM and X-ray combined analysis approach allowing to work with the real shell!

↳ SEM studies : 3 crossed lamellar layers of biogenic aragonite

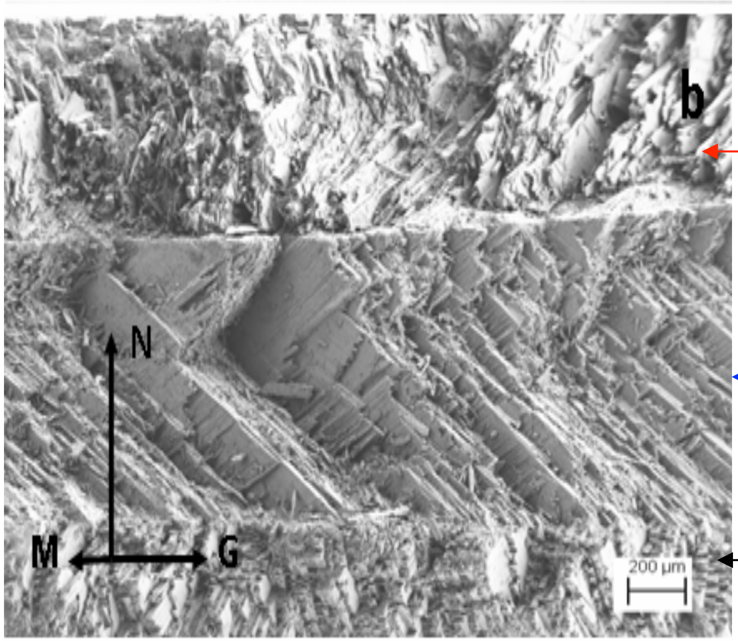

OCL : Outer Comarginal Crossed Lamellae : lamellae plane // M

IRCL : Intermediate Radial Crossed Lamellae : lamellae plane ⊥ M

ICCL : Inner Irregular Complex Crossed Lamellae

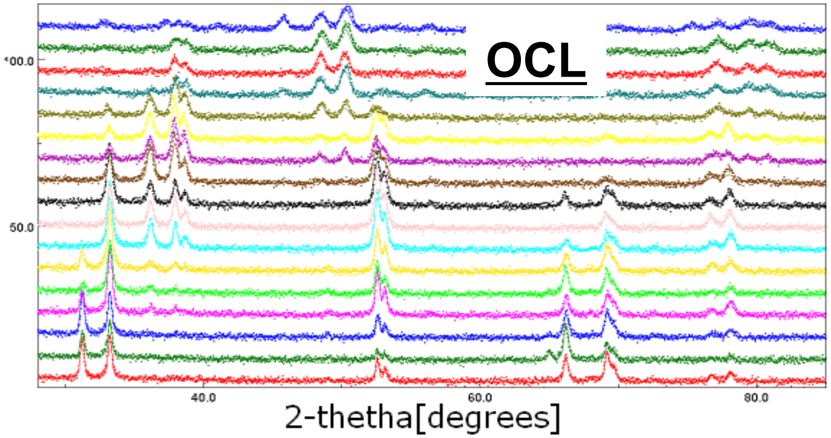

e scanning grid of 5°x5° -> 936 X-ray

Pure aragonite reference cell parameters :

(no residual stress evidenced)

a = 4.9623(3) Å, b = 7.968(1) Å, c = 5.7439(3) Å

↓

n : texture, cell parameters, atomic

lated to aplanarity of CO_3 groups.

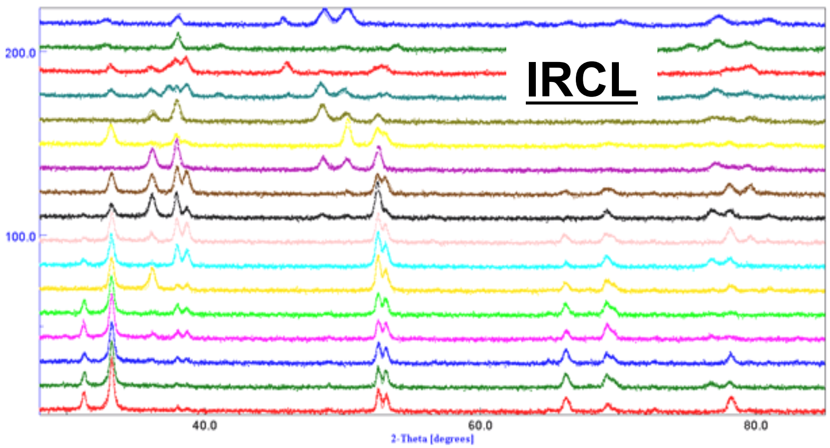

layer		OCL	IRCL	ICCL
a (Å)		4.98563(7)	4.97538(4)	4.9813(1)
b (Å)		8.0103(1)	7.98848(8)	7.9679(1)
c (Å)		5.74626(3)	5.74961(2)	5.76261(5)
ΔV/V		1.05 %	0.62 %	0.71 %
OD maximum (m.r.d.)		299	196	2816
OD minimum (m.r.d.)		0	0	0
Texture index (m.r.d.^{2})		42.6	47	721
OD reliability factors	R_w (%)	14.3	11.2	32.5
	R_B (%)	15.6	12.7	47.8
Rietveld reliability factors	GoF (%)	1.72	1.72	3.05
	R_w (%)	29.2	28.0	57.3
	R_B (%)	22.9	21.7	47.2
	R_{exp}(%)	22.2	21.3	32.8

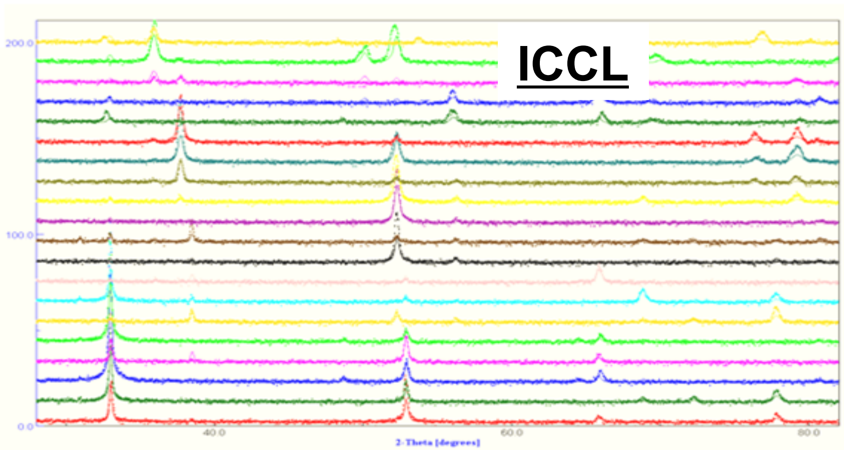

Largest crystallite organisation closer to the animal

Recalculated pole figures

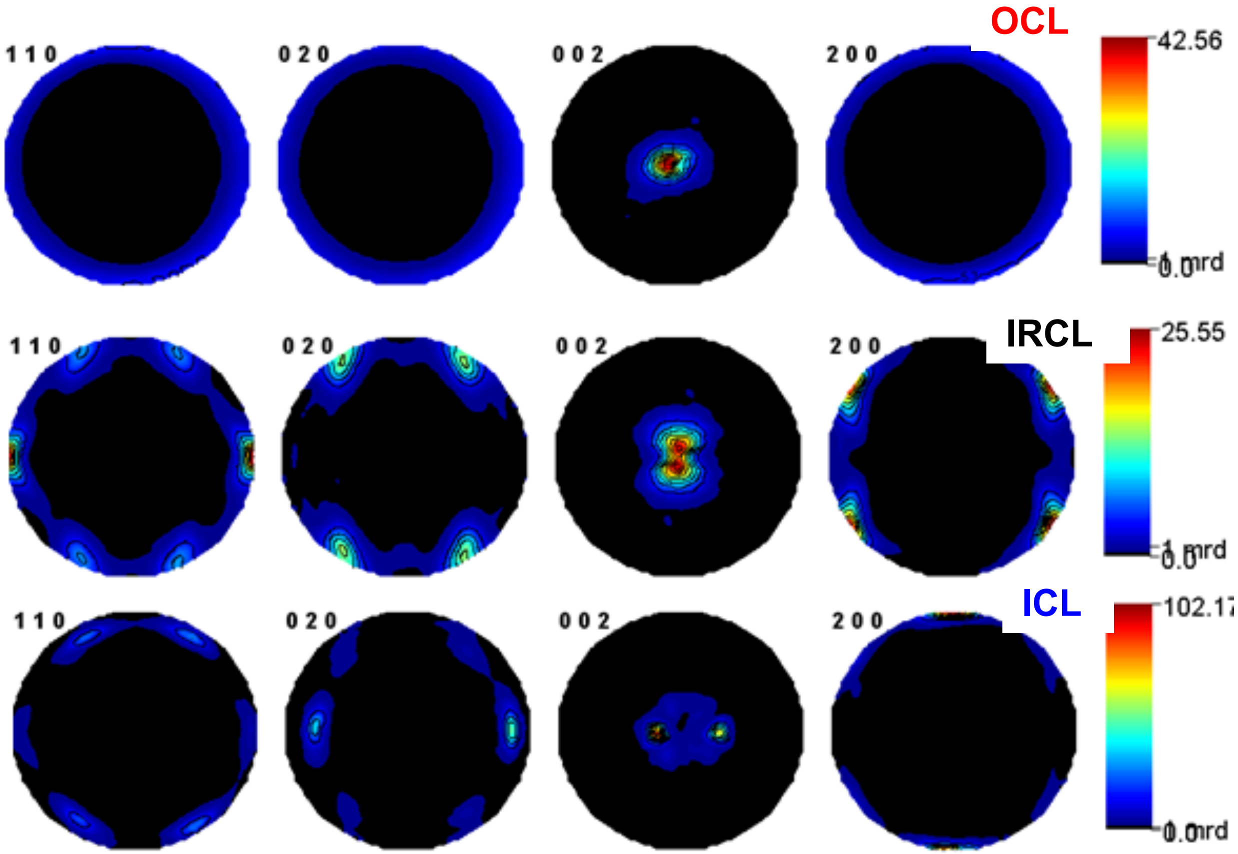

Fiber texture: $\vec{c}$ // N

Split of $\vec{c}$ axes around N
+ two contributions //
(G,N) plane.

Split of $\vec{c}$ axis from N
+ two contributions //
(M,N) plane.

Texture information coherent with usually admitted gastropods phylogeny for this taxon !

<u>Combined analysis</u> : access to cell parameters and distorsion of aragonite shell without needs of powdering specimen !!

		Geological reference	*Charonia lampas* OCL	*Charonia lampas* IRCL	*Charonia lampas* ICCL
a (Å) b (Å) c (Å)		4.9623(3) 7.968(1) 5.7439(3)	4.98563(7) 8.0103(1) 5.74626(3)	4.97538(4) 7.98848(8) 5.74961(2)	4.9813(1) 7.9679(1) 5.76261(5)
Ca	y z	0.41500 0.75970	0.41418(5) 0.75939(3)	0.414071(4) 0.76057(2)	0.41276(9) 0.75818(8)
C	y z	0.76220 -0.08620	0.7628(2) -0.0920(1)	0.76341(2) -0.08702(9)	0.7356(4) -0.0833(2)
O1	y z	0.92250 -0.09620	0.9115(2) -0.09205(8)	0.9238(1) -0.09456(6)	0.8957(3) -0.1018(2)
O2	x y z	0.47360 0.68100 -0.08620	0.4768(1) 0.6826(1) -0.08368(6)	0.4754(1) 0.68332(9) -0.08473(5)	0.4864(3) 0.6834(2) -0.0926(1)
ΔZ_{C-O1} (Å)		0.05744	0.00029	0.04335	0.1066

ΔZ_{C-O1} ↗ from outer to inner layer correlated to the organic macromolecules presence + coherent with the ↘ of texture strength → control loss from macromolecules on aragonite stabilization farther from animal!

Anisotropic cell distorsions yet observed in biogenic aragonite powderised layers

b) *Pinctada maxima*:

shell nacre of giant oyster =
biomaterial that stimulates bone regeneration + in vivo studies show its biocompatibility and that nacre also able to induce new bone formation

➢ **Geological nacre composition = pure aragonite (orthorhombic Pmcn)**
Microstructure = strongly textured pseudo hexagonal nacre tablets

➢ ***Pinctada maxima* nacre = aragonite and organic phases (2% – 5%) : biogenic nacre**

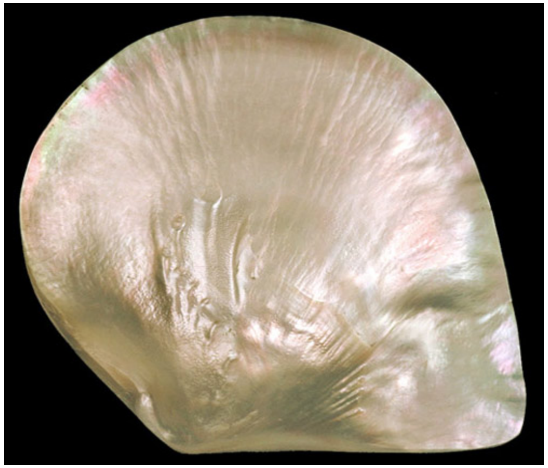

Pinctada maxima

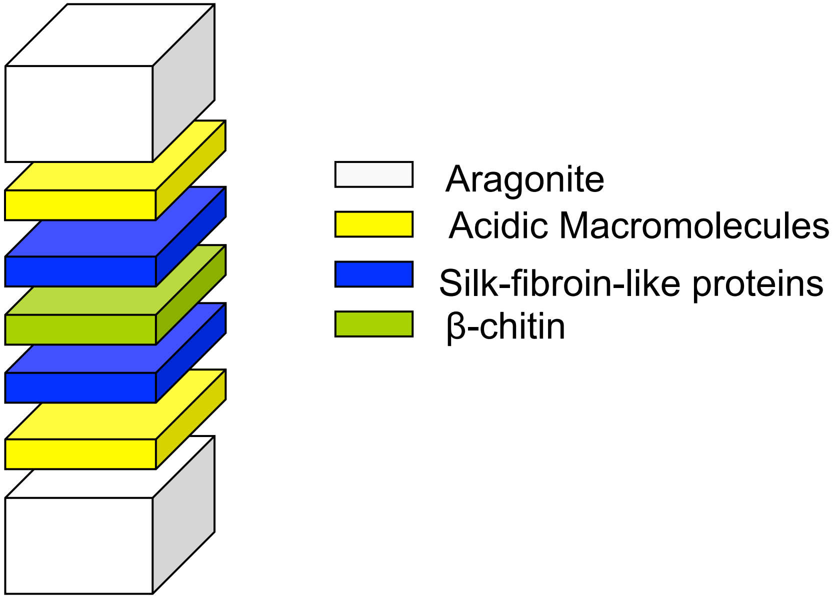

X-ray Combined analysis approach : 2.5°*2.5° grid
Better understanding of the "natural" nacre structure and microstructure in order to deposit synthetic nacre

		Geological reference	*Pinctada maxima*
a (Å)		4.9623(3)	4.97071(4)
b (Å)		7.968(1)	7.96629(6)
c (Å)		5.7439(3)	5.74804 (2)
Ca	y	0.41500	0.41479 (3)
	z	0.75970	0.75939 (2)
C	y	0.76220	0.7676 (1)
	z	-0.08620	-0.0831 (1)
O1	y	0.92250	0.9134 (1)
	z	-0.09620	-0.09255 (7)
O2	x	0.47360	0.4678 (1)
	y	0.68100	0.68176 (7)
	z	-0.08620	-0.09060 (4)
ΔZ_{C-O1} (Å)		0,057	0,054

Cell parameter distorsions due to the presence of organic molecules like in *Charonia lampas*

$R_w = 21.95\%$
$R_B = 24.92\%$

Weak distorsion of the CO_3 group

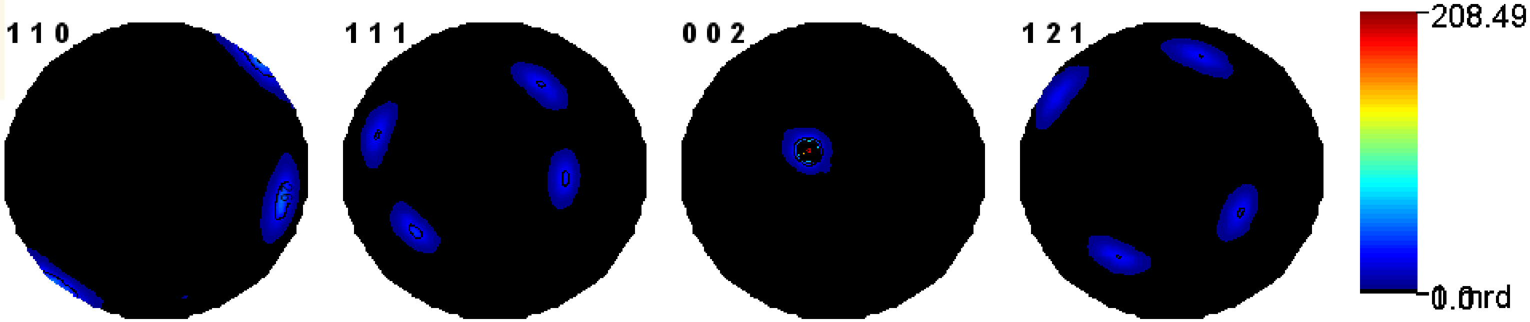

Normalized pole figures : strong texture with c-axis orientation weakly tilted from the normal shell

Nacre tablets of *Pinctada maxima* perfectly aligned with shell large domains showing common alignment of c-axes resembling a single-crystal or textures observed in epitaxial films :

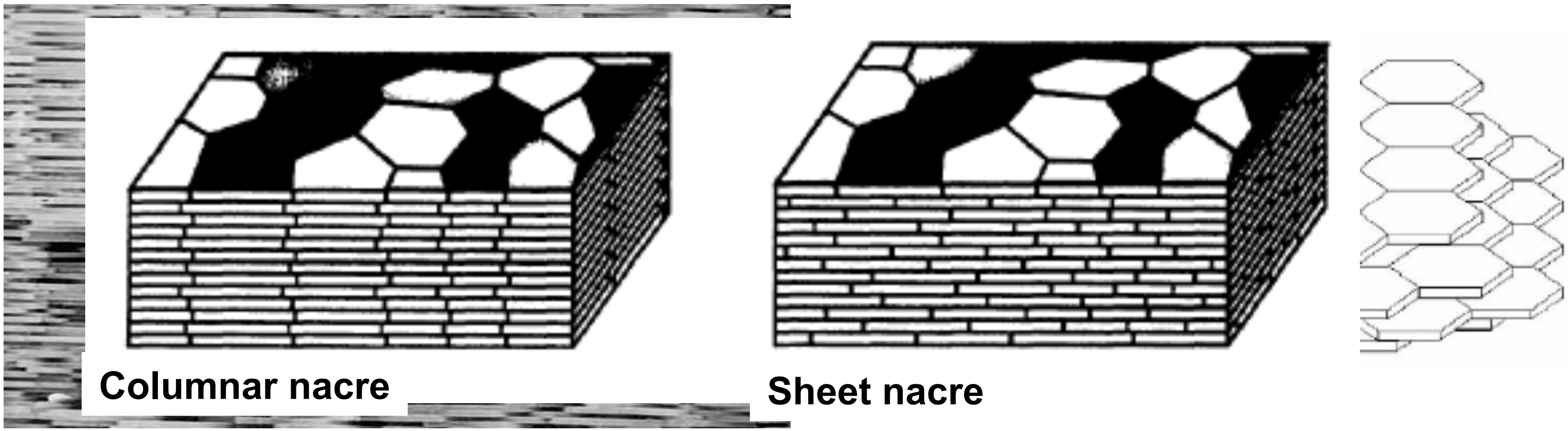

MEB cross section image showing the *Pinctada maxima* brick wall nacre (sheet nacre)

Observed texture ≠ from the columnar nacre evidenced in some gastropod (fiber textures) and Cephalopoda (double “twinned” textures) shells

↳ Illustration of the X-ray combined analysis approach

4) Biomimetic $CaCO_3$: Electrodeposited aragonite
(Thesis of C. Krauss)

Medical european law: forbids animal proteins in human body
→ mimic textured hexagonal like aragonite

↳ synthetic nacre for osteopathy on Ti substrate:

- **prostheses mainly in titanium subjected to bone resorption**
- **Ti susbtrate : high strength, inertia and immunity to corrosion**

↳ $CaCO_3$: 3 allotropic forms

- **Calcite (R3c - trigonal): too much stable form but non osteoinductive**
- **Vaterite (P63/mmc - hexagonal): non-stable form not good for applications**
- **Aragonite (Pmcn - orthorhombic): metastable form ; Gibbs energy ΔG_0(C->A) = -1kJ/mol**

↓

Electrodeposition of $CaCO_3$ in aragonitic form on titanium foil
+ microstructure and texture caracterizations: SEM and X-Ray diffraction

# of deposited aragonite on Ti foils

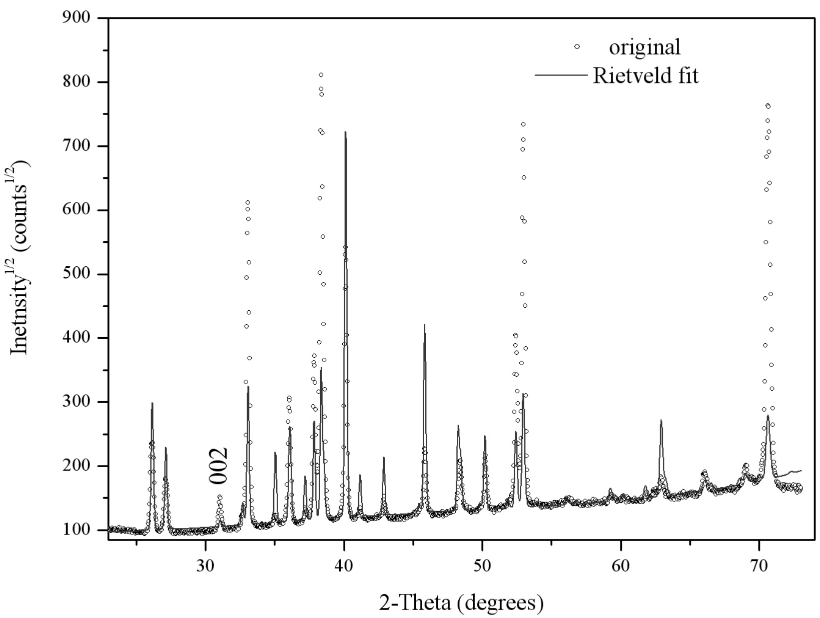

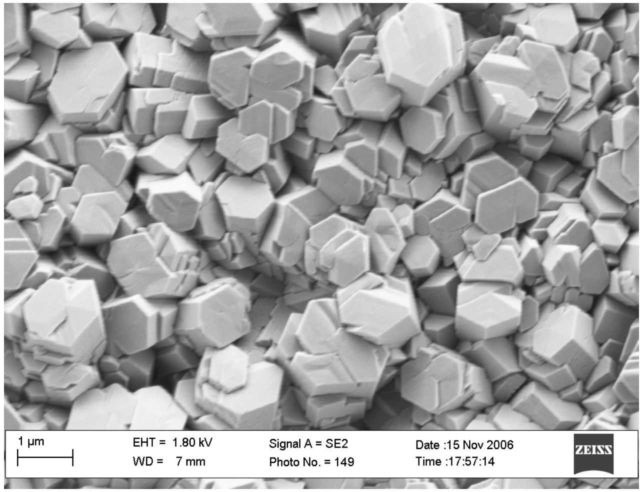

Nonoptimized deposited films: cauliflower-shaped aragonite + calcite + vaterite

Corresponding X-ray diagram: only aragonite is evidenced with a pronounced (00l) texture

Optimized deposited films with nacre like pseudo hexagonal shaped crystals

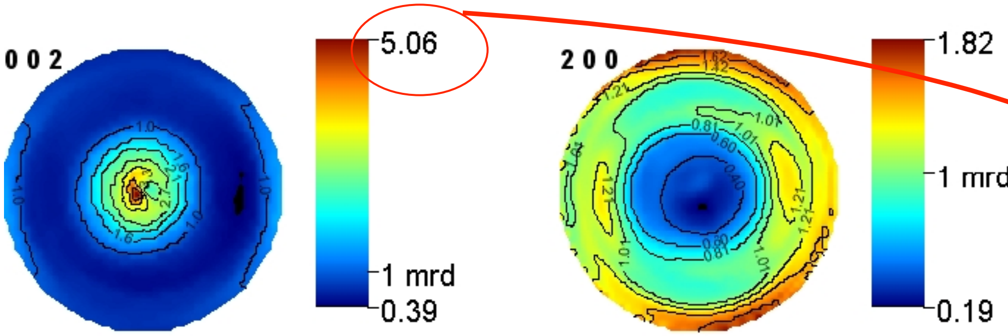

Texture strength far from natural nacre → differences can be associated to organic driven processes

Recalculated pole figure : <00l> fiber like texture

Addition of Pinctada maxima organic molecules to the electrolyte:

2 types of organic phases (polar and apolar)

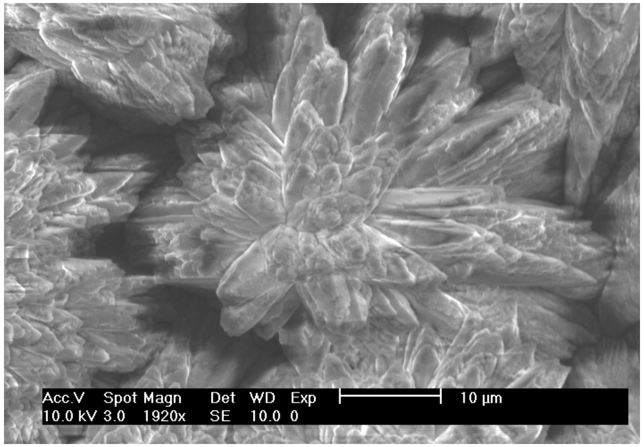

Apolar phase **: cauliflower-shaped aragonite + calcite + vaterite**

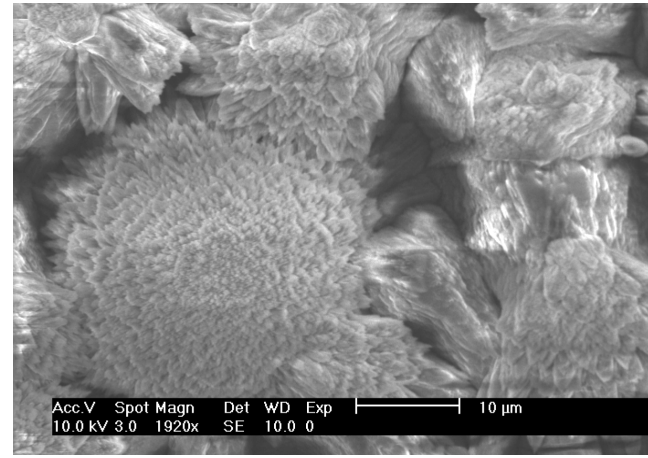

Polar phase **: compact cauliflower-shaped aragonite + calcite + vaterite**

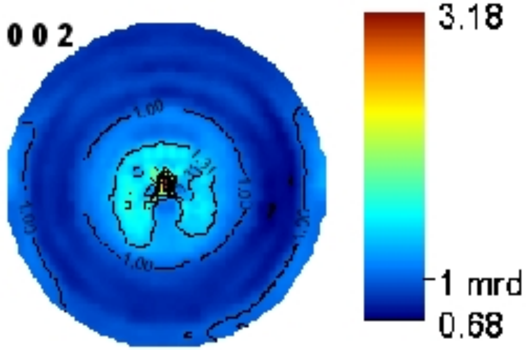

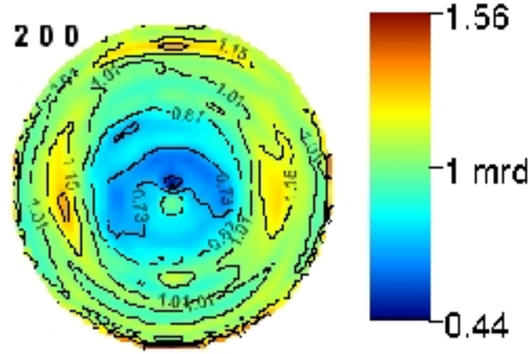

Unexpected reduction of the <00l> texture !

Crystallite shape and texture strength must be improved!

↳ Illustration of the X-ray combined analysis approach

5) Biomimetic $CaCO_3$: synthesis of $CaCO_3$ polymorphs with polyacrylic acid (PAA)
(S. Ouhénia thesis – december 2008)

↳ Some studies show that surfactants can influence $CaCO_3$ nucleation, growth and grain shapes and consequently control crystal phases formation not usually stabilized under natural environment.

↳ Aragonite (nacre) metastable at room temperature transforms to calcite in natural environment.

↓

Many attempts to mimic aragonite, biological synthesis using different organic substrates and additives : for example aragonite thin films form on polyvinyl alcohol matrices in presence of polyacrilic acid (PAA)….

↳ This work: $CaCO_3$ crystallization from aqueous solutions in presence of PAA at various temperatures (25°C to 80°C).
PAA's effects studied by SEM and X-ray diffraction.

At 25°C with and without PAA

Vaterite

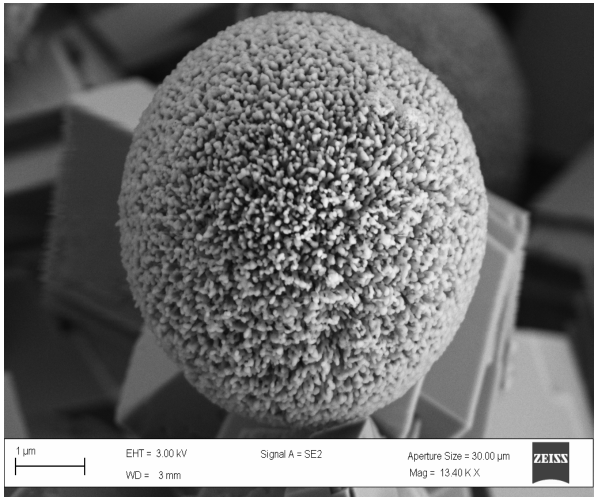

Spherical particles : 3µm

Without PAA

Calcite

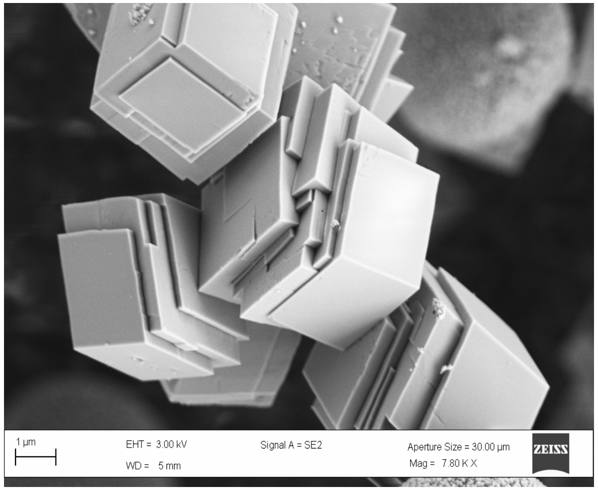

Rhombic interpenetrated

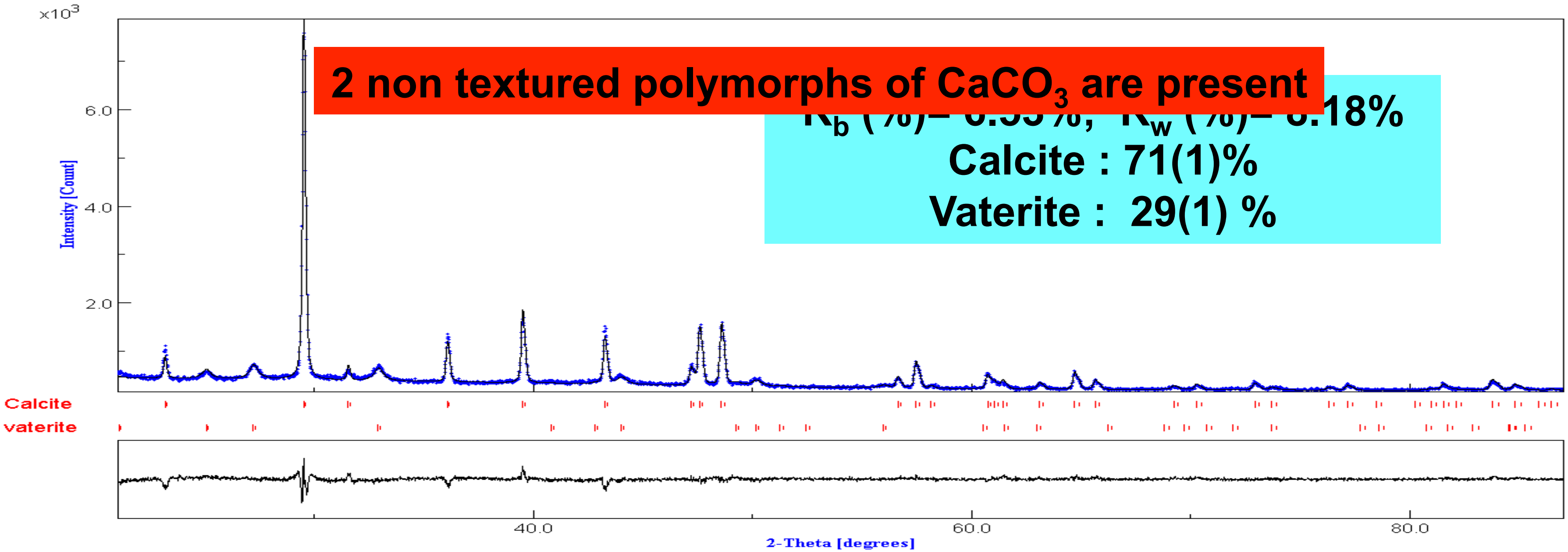

Biomimetic $CaCO_3$

At 25°C with and without PAA

Vaterite

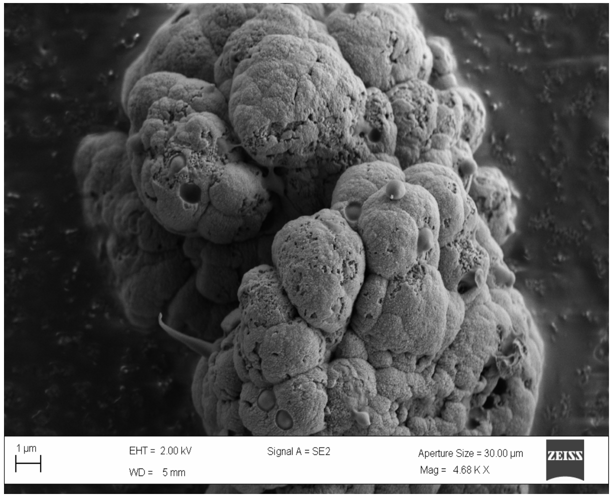

Deformed spheres agglomerated in raspberry particles :15 μm

With PAA

Calcite

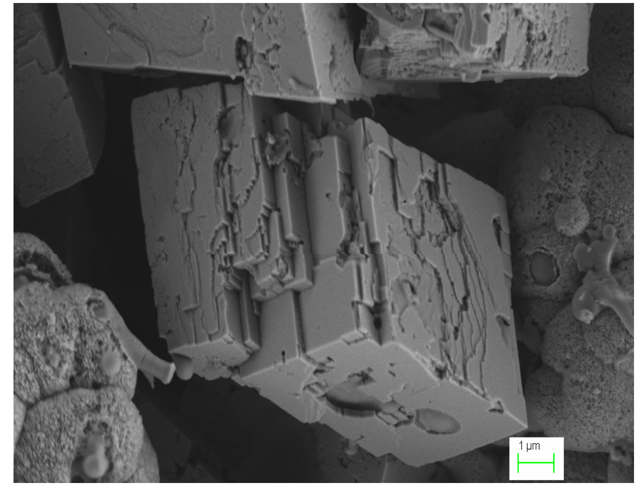

Rhombic particles with less regular faces and porosity : 10 μm

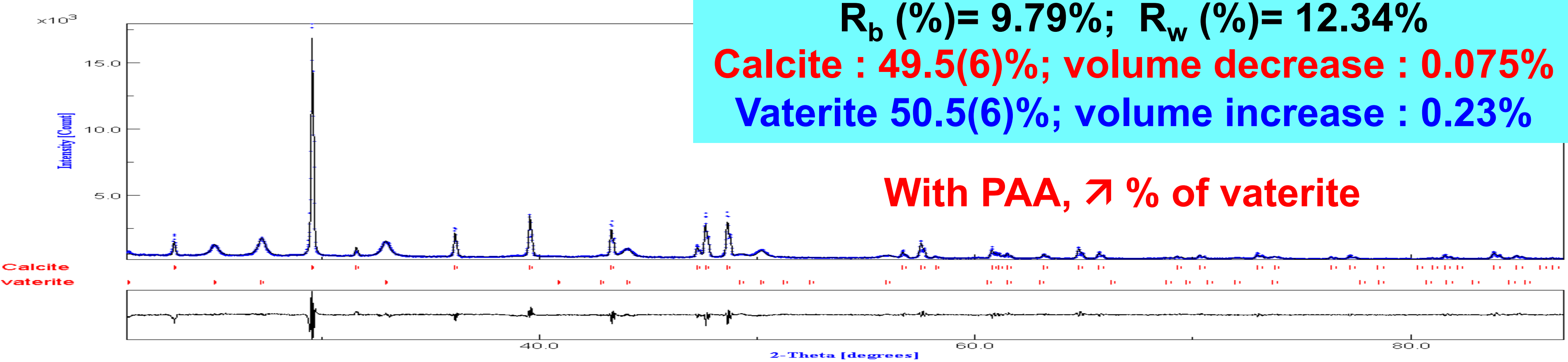

R_b (%)= 9.79%; R_w (%)= 12.34%

Calcite : 49.5(6)%; volume decrease : 0.075%

Vaterite 50.5(6)%; volume increase : 0.23%

With PAA, ↗ % of vaterite

At 50°C without PAA

Vaterite : raspberries	Calcite : regular rhombs	Aragonite: califlowers
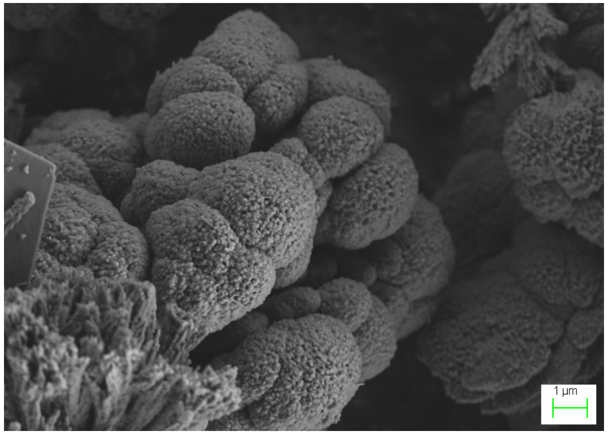	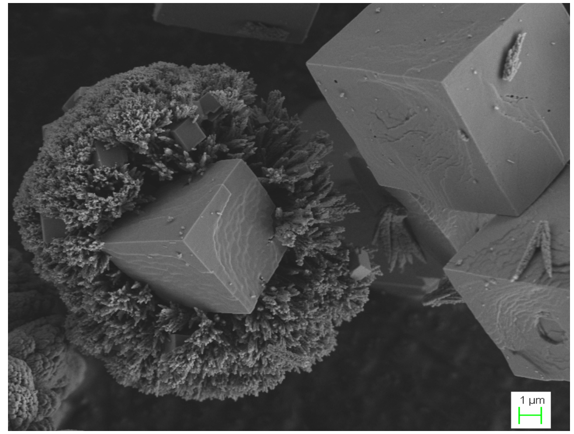	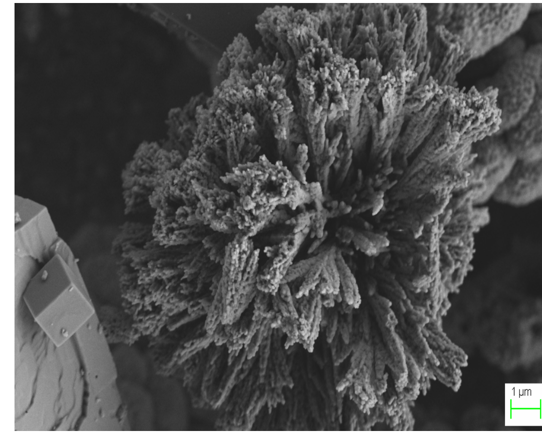

3 non textured polymorphs of $CaCO_3$ are present + anisotropic crystallite shape → Popa formalism

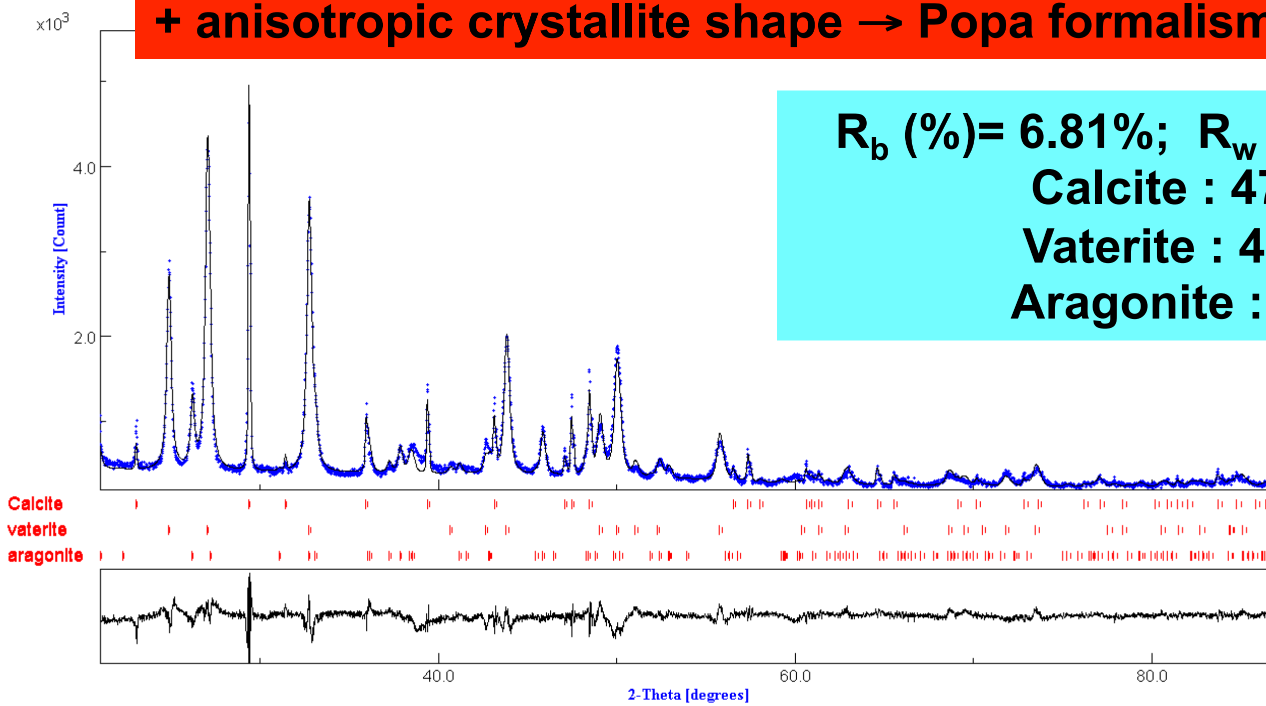

R_b (%)= 6.81%; R_w (%)= 8.40%
Calcite : 47%
Vaterite : 46%
Aragonite : 7%

At 50°C with PAA

Vaterite flowers | **Calcite : porous rhombs** | **Aragonite : dendrites**

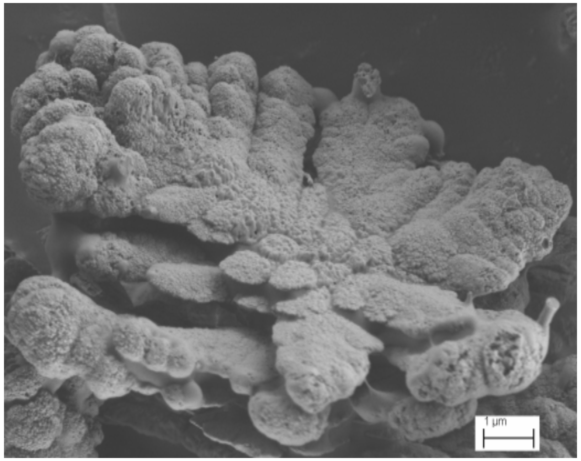

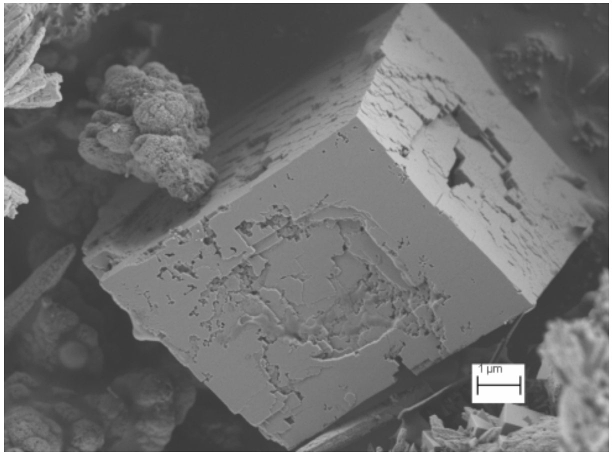

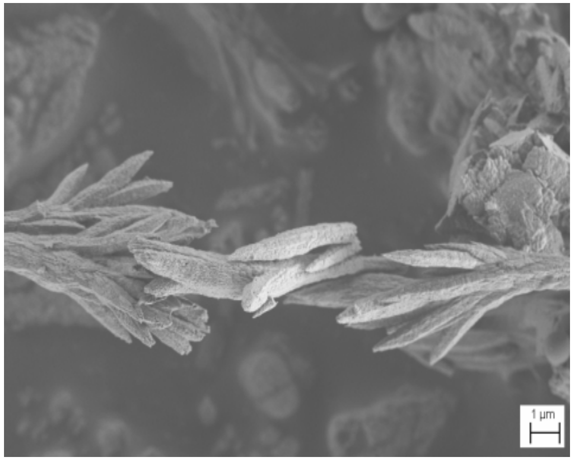

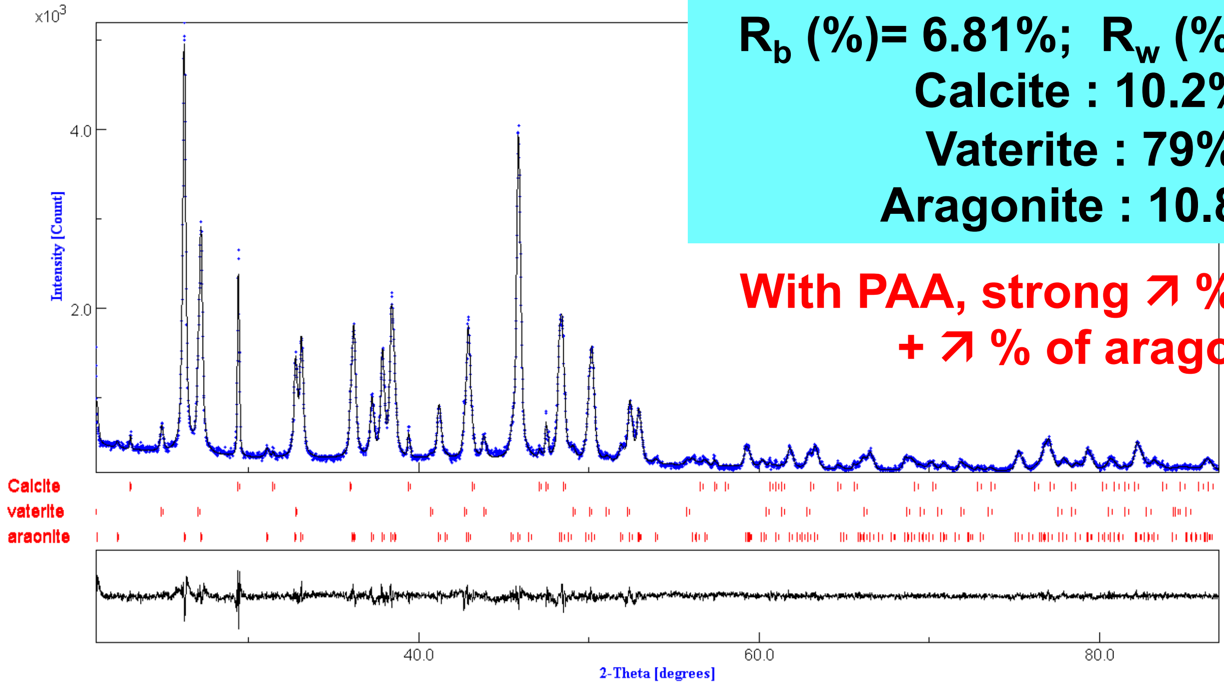

R_b (%)= 6.81%; R_w (%)= 8.40%
Calcite : 10.2%
Vaterite : 79%
Aragonite : 10.8%

With PAA, strong ↗ % of vaterite + ↗ % of aragonite

Anisotropic crystallite shapes at 50°C without and with PAA

	Vaterite	Aragonite	Calcite
Without PAA	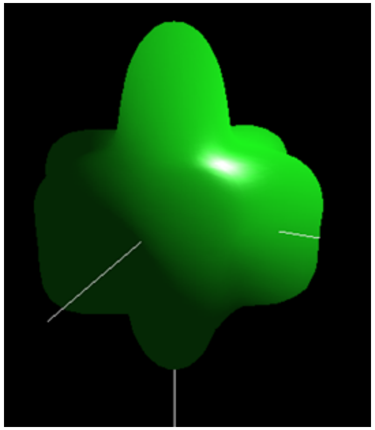 c-elongated needles with c/a ~ 0.76	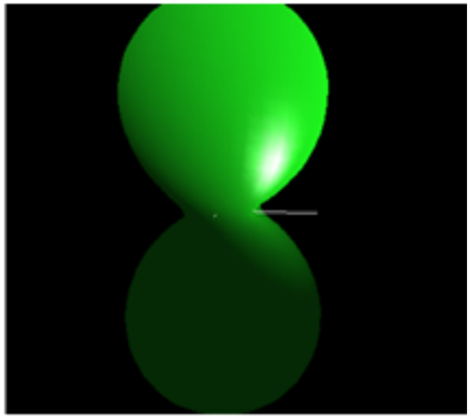 c-elongated needles with c/b ~ 0.11	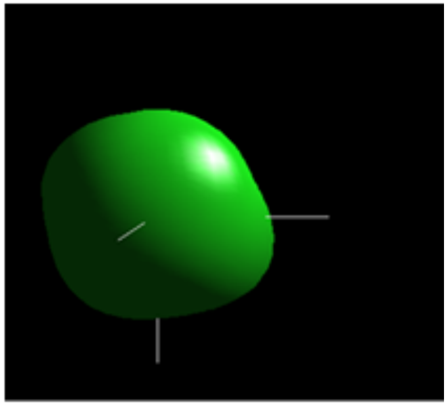 Quasi-cubic crystallites
With PAA	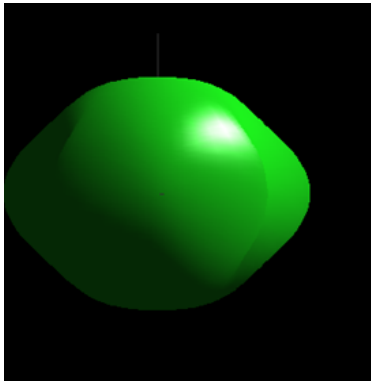 flatness along c-axis with c/a ~ 1.36 Idem aragonite!	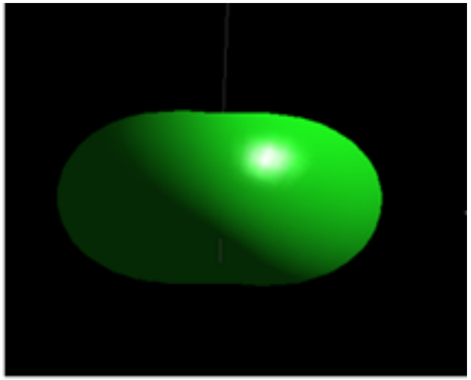 Ca-PAA complex adsorption on carbonate group faces blocks growth along c-axis + prevents transformation in calcite !	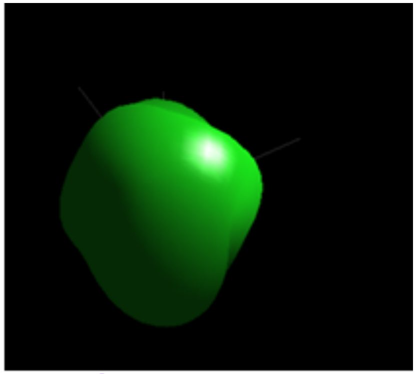 Quasi-cubic crystallites → no site for Ca-PAA complex adsorption

At 80°C without PAA

Acicular aragonite

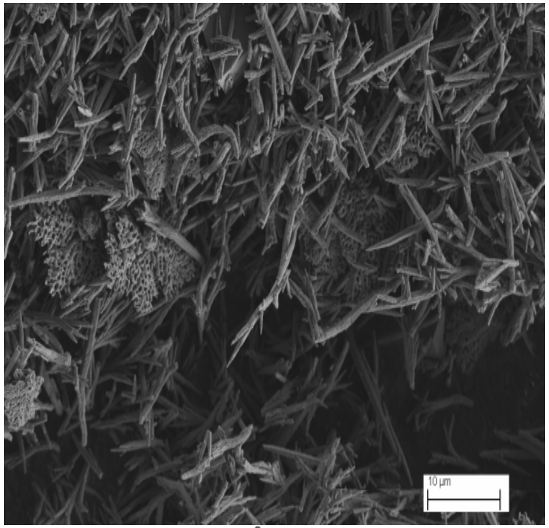

Vaterite sponges

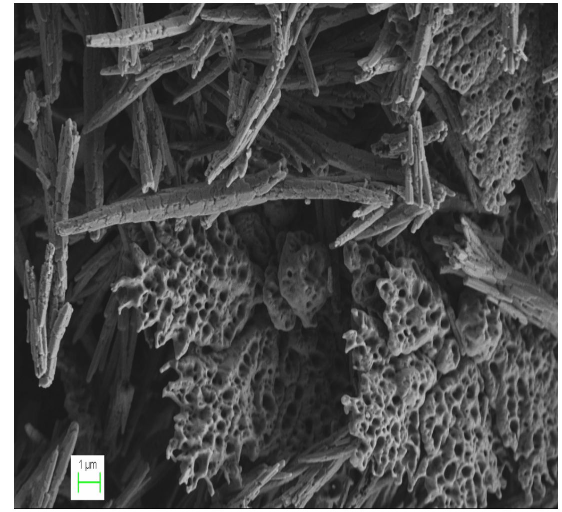

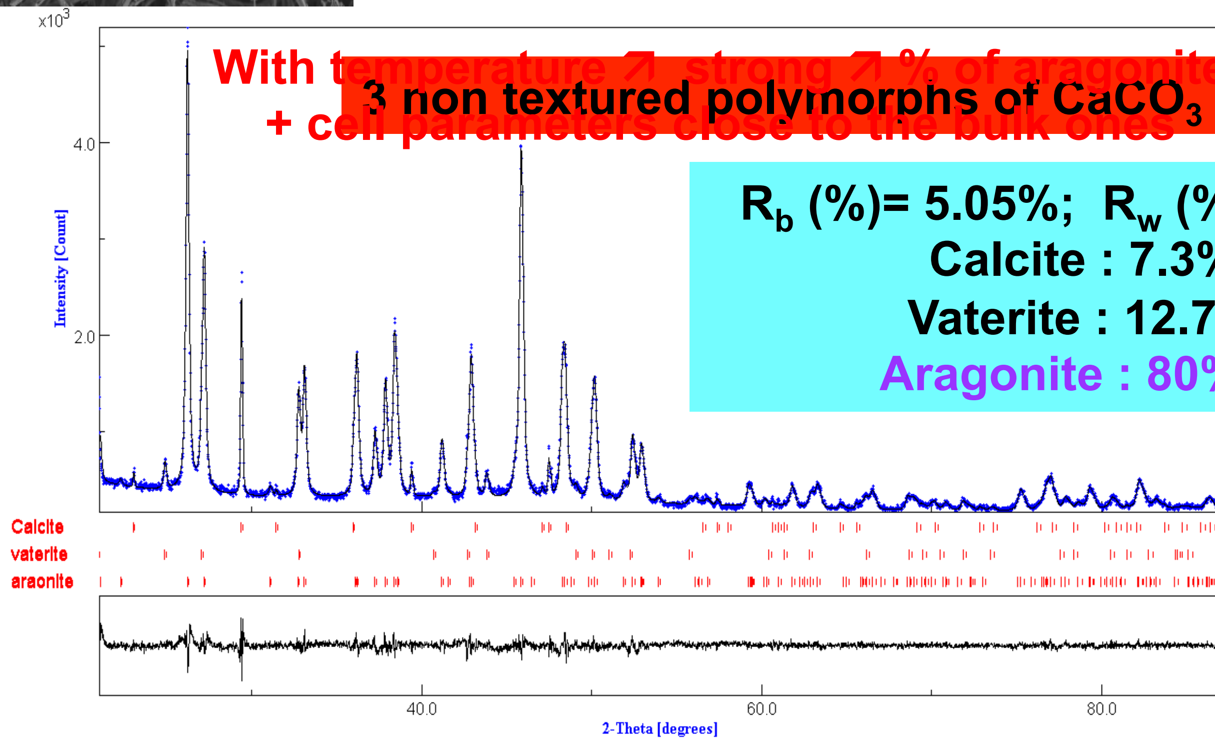

With temperature ↗ strong ↗ % of aragonite
+ cell parameters close to the bulk ones

3 non textured polymorphs of $CaCO_3$ are present

R_b (%)= 5.05%; R_w (%)= 6.86%
Calcite : 7.3%
Vaterite : 12.7%
Aragonite : 80% !!

At 80°C with PAA

SEM backscattered images:
only aragonite needles are observed

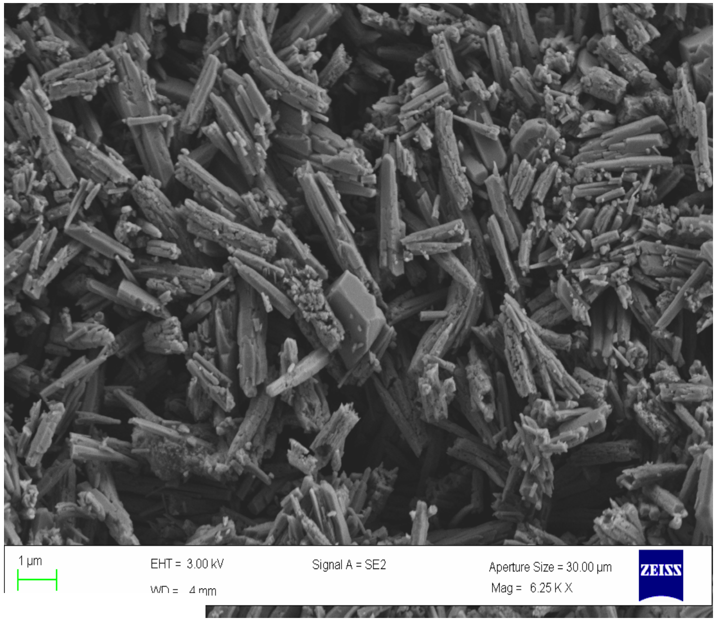

3 non textured polymorphs of $CaCO_3$ are present

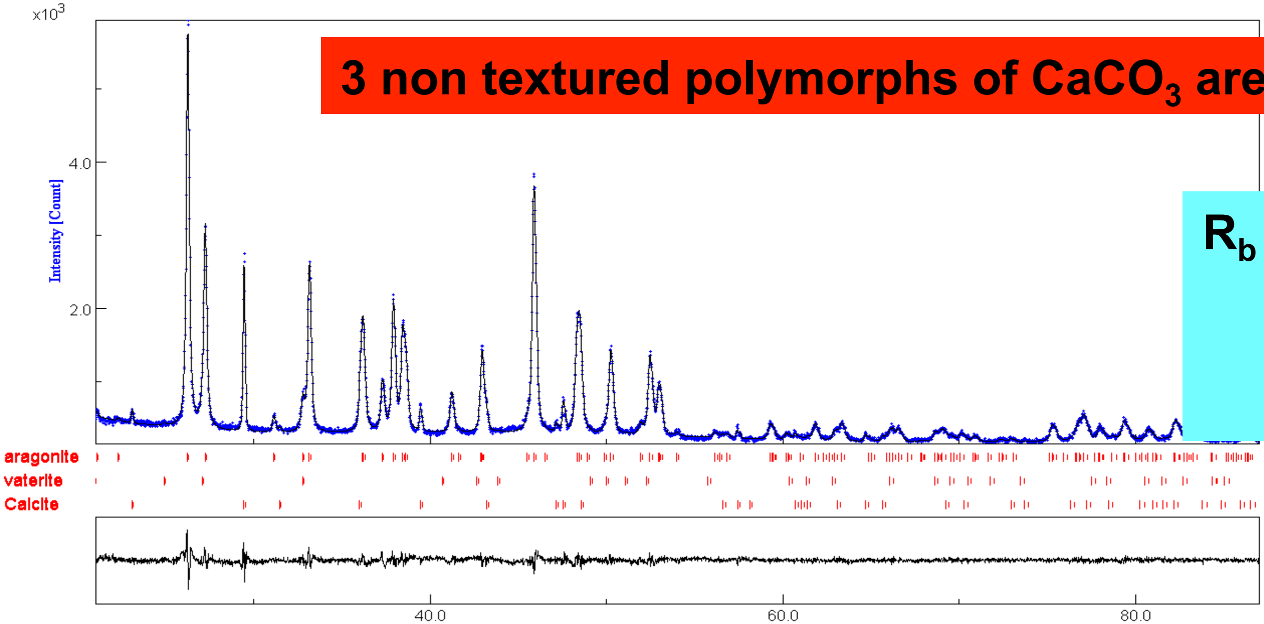

R_b (%)= 7.25%; R_w (%)= 9.17%
Calcite : 8.5%
Vaterite : 1.5%
Aragonite : 89% !!

With PAA, ↘ % of vaterite + ↗ % of aragonite

Conclusions: PAA and temperature ↗ favor non textured aragonite growth : shift of chemical equilibrium of 3 polymorphs!

↳ Illustration of the neutron combined analysis approach

6) Texture and phylogeny of mollusc shell fossils: *Belemnite* rostrum

Shell fossils : phylogenetic evolution determination + specifications of stratigraphic age of geological formations.

↳ **Belemnite rostrum = common name applied to an extinct order (Belemnoida) of molluscs belonging to the Cephalopoda (like squids, octopuses, and *Nautilus*).**

↳ **greatest abundance and diversity during the Jurassic and Cretaceous periods.**

↳ ***Belemnites* ranged at the largest genetic distance from actually measured species + can serve as an outgroup for a phylogenetic classification.**

↳ **The most common fossilised part of the internal shell = "rostrum" consists of massive calcite. The rostrum served as a counter-weight to the buoyancy provided by the chambered shell and also for protection of that delicate shell.**

Quantitative Texture Analysis provides a set of new characters usable as a complement for a phylogenetic interpretation in cladistic or phenetic approaches

+

in case of calcitic shell layers QTA is able to link extinct and living molluscs via fossilised species!

Morales et al.(2002), Mat. Sci. For. 408, 1687

↳ Presence of **large grains** (sizes range from few cm to over 1 meter for *Belemnitae americanus*) → **X-ray diffraction can't properly probe texture !!**

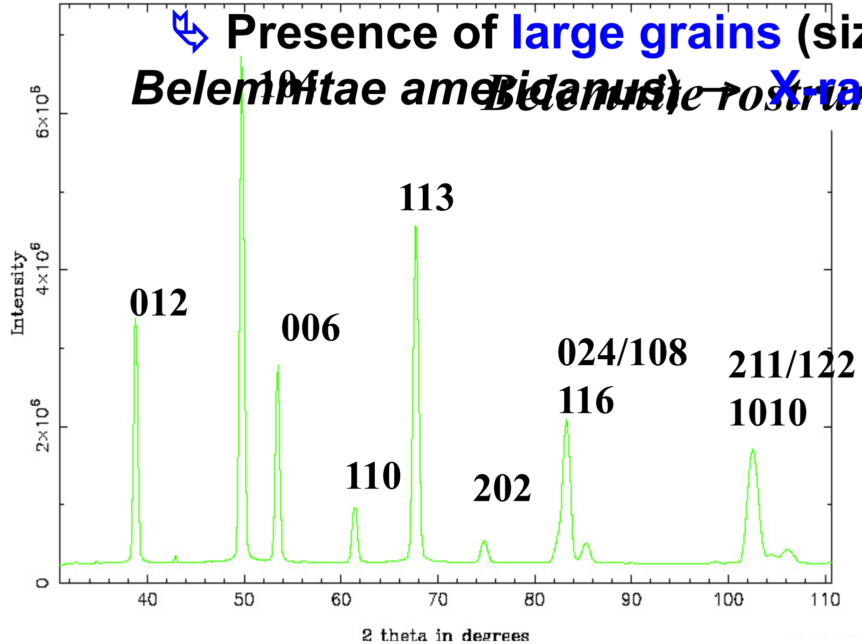

Neutron diagram (D1B-ILL line): sum over 1368 scans over as many sample orientations.

↓

Pure calcite is observed

Intra-phase peak overlaps + texture → combined analysis approach

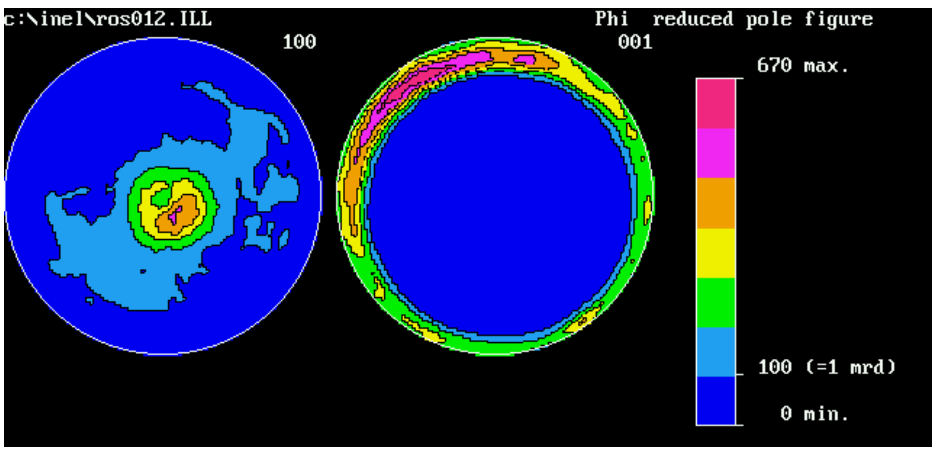

Main pole figures: As in other cephalopod, calcite c-axes randomly distributed around belemnite rostrum cylindrical axis .

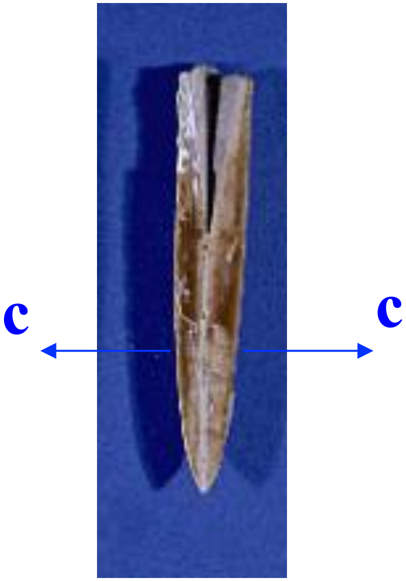

Correlated to the c-axes of *Nautilus sp.* aragonite layers → **Nacre not ancestral** and might have evolved from original calcite : on the contrary of the common hypothesis !

↳ Combined analysis approach actual limitations:

7) Multiphased Cr^{2+}:ZnSe films: texture, anisotropic crystallite sizes, residual stresses , twin faults and phase analysis

Mid- IR region (2 – 5 µm) « molecular figerprint region » → environmental, medecine, biological and defense applications

- 1996 : transition-metal doped II-VI zinc chalcogenide compound for room-temperature laser materials in the mid-IR.

Best candidate = Cr^{2+}: ZnSe

➤ Cr^{2+}:ZnSe films → Realization of compact optically and electrically pumped mid-IR micro-lasers.

↓

fluorescence and stimulated emission optimization = production of quality films

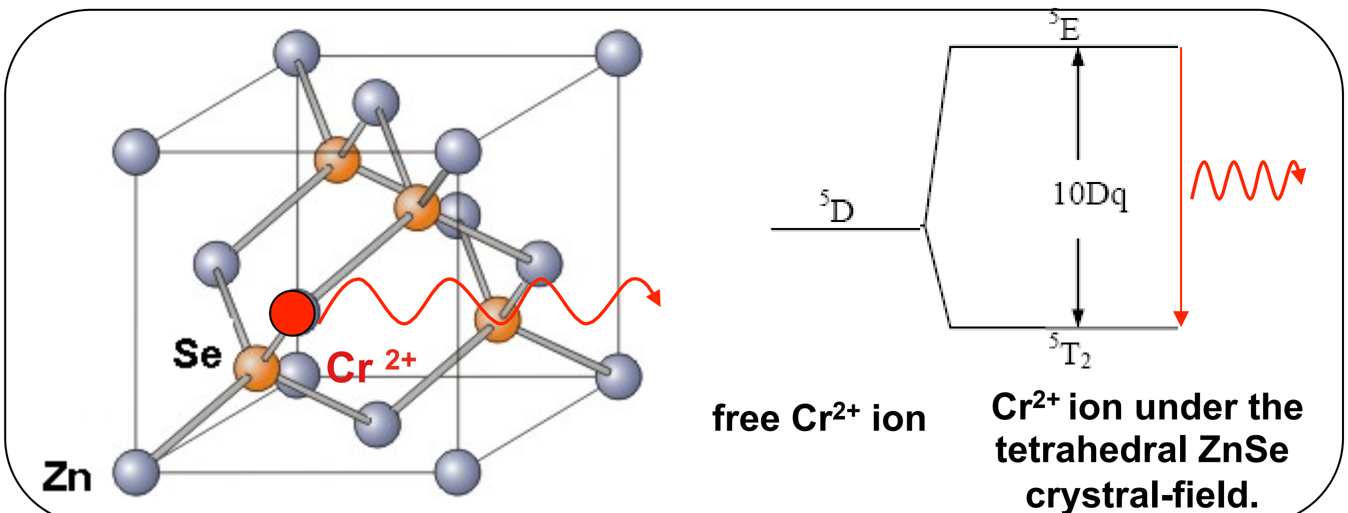

↳ RX θ-2θ diagrams

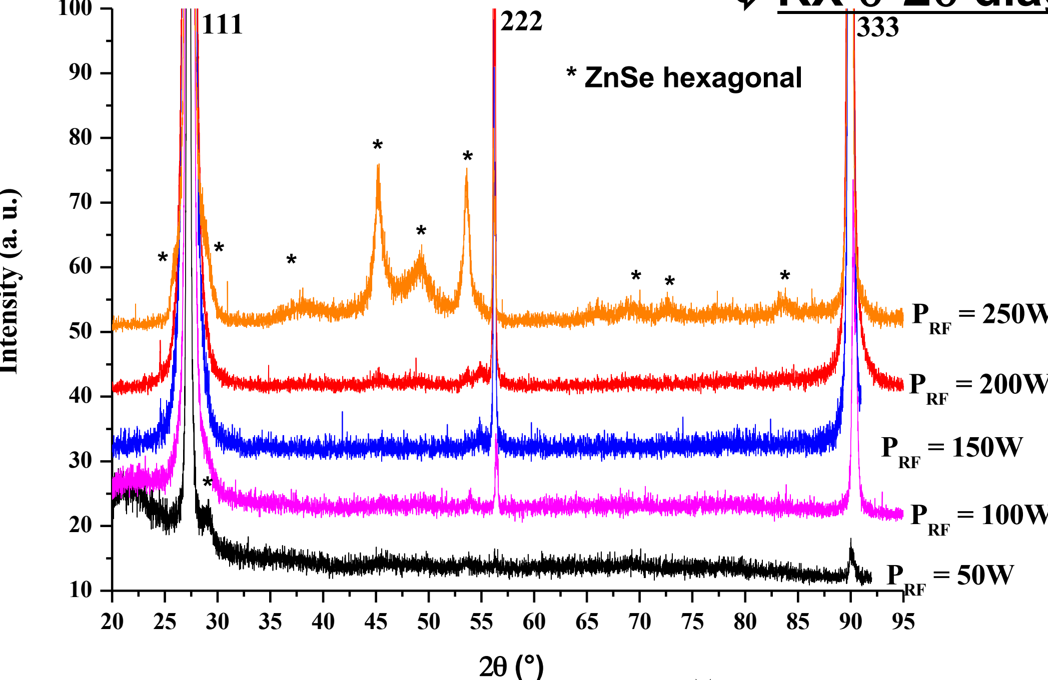

- cubic (C) and hexagonal (H) ZnSe
- H-ZnSe more marked at higher P_{RF}
- highly textured with in majority $<111>_{C\text{-}ZnSe}$ // $\vec{n}_{film}$

↳ χ-scans with ω =13.65°

Anisotropic crystallite shapes

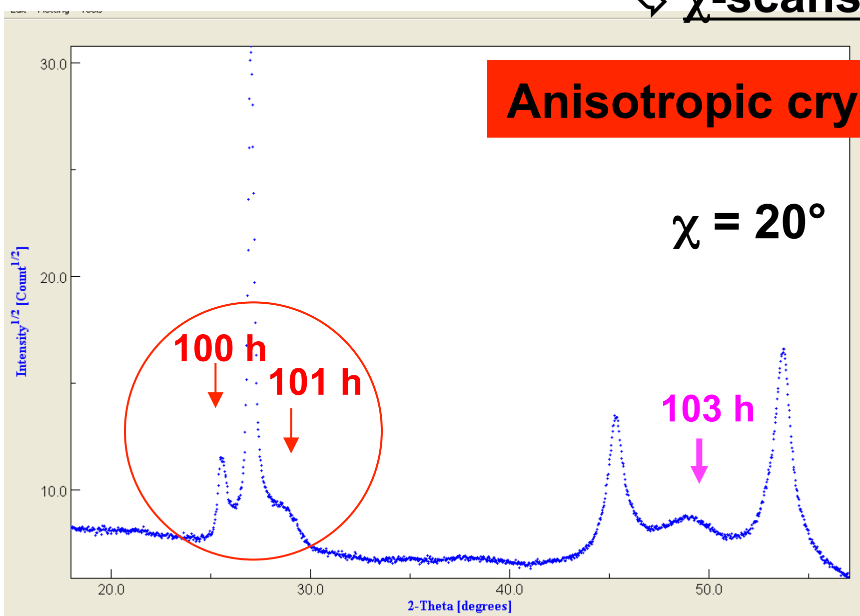

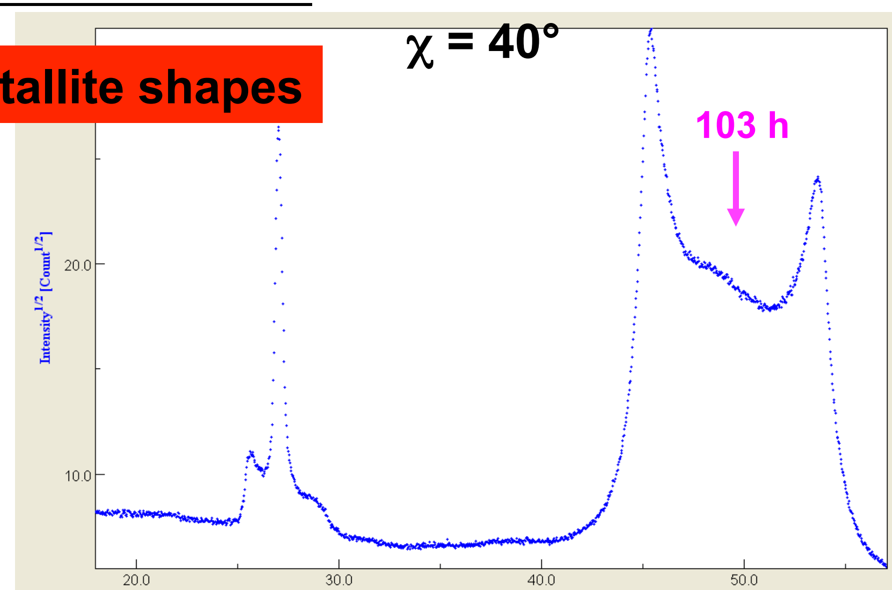

Multiphased Cr^{2+}:ZnSe films : combined analysis approach actual limitations

ω =13.65°, P_{RF} = 200W

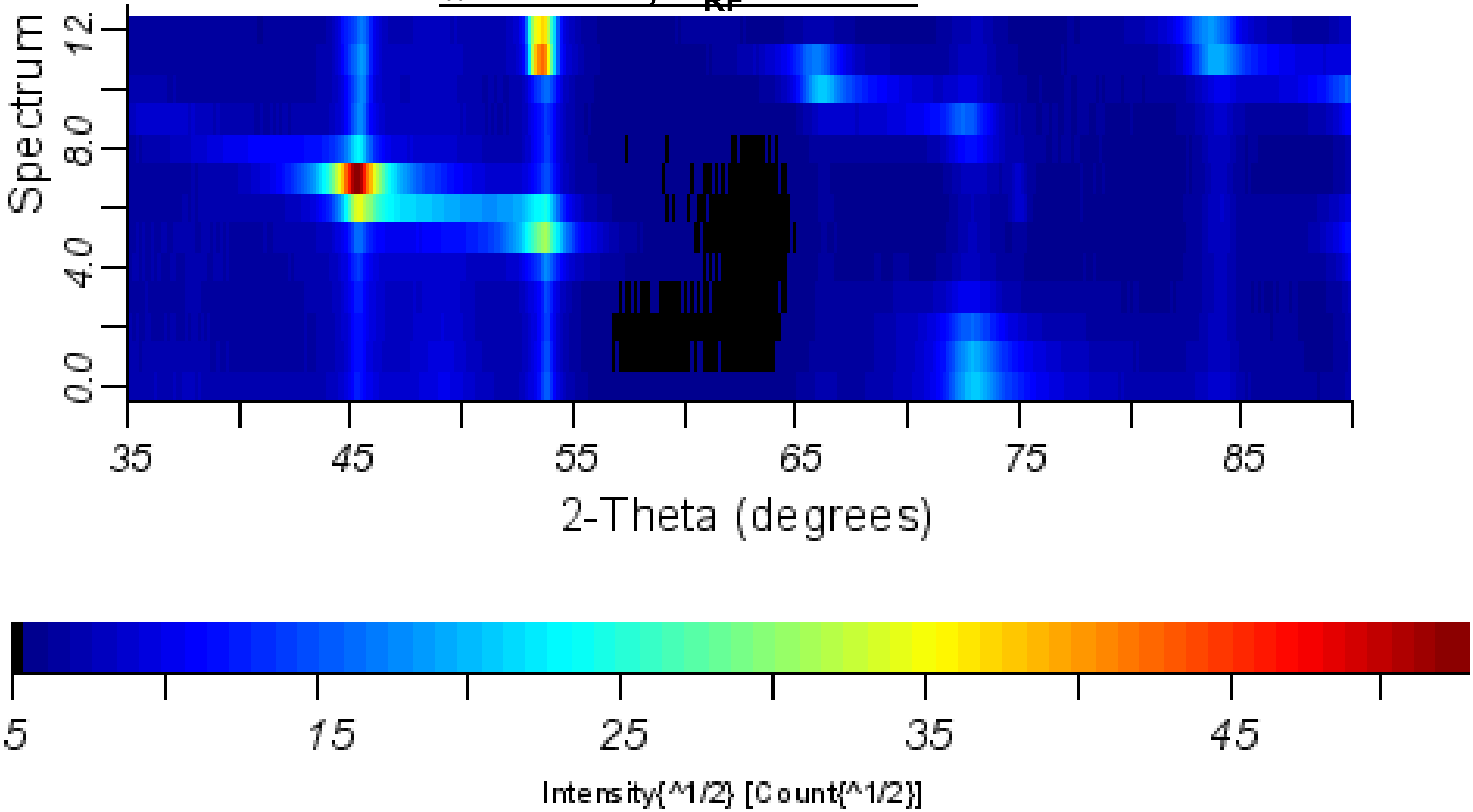

Residual strains for both C-ZnSe and H-ZnSe !
Biaxial model with $\sigma_{11} = \sigma_{22}$ due to fibre like texture

Fibre strong textures + 2 phases + anisotropic crystallite shape + residual strains → combined analysis approach is necessary!

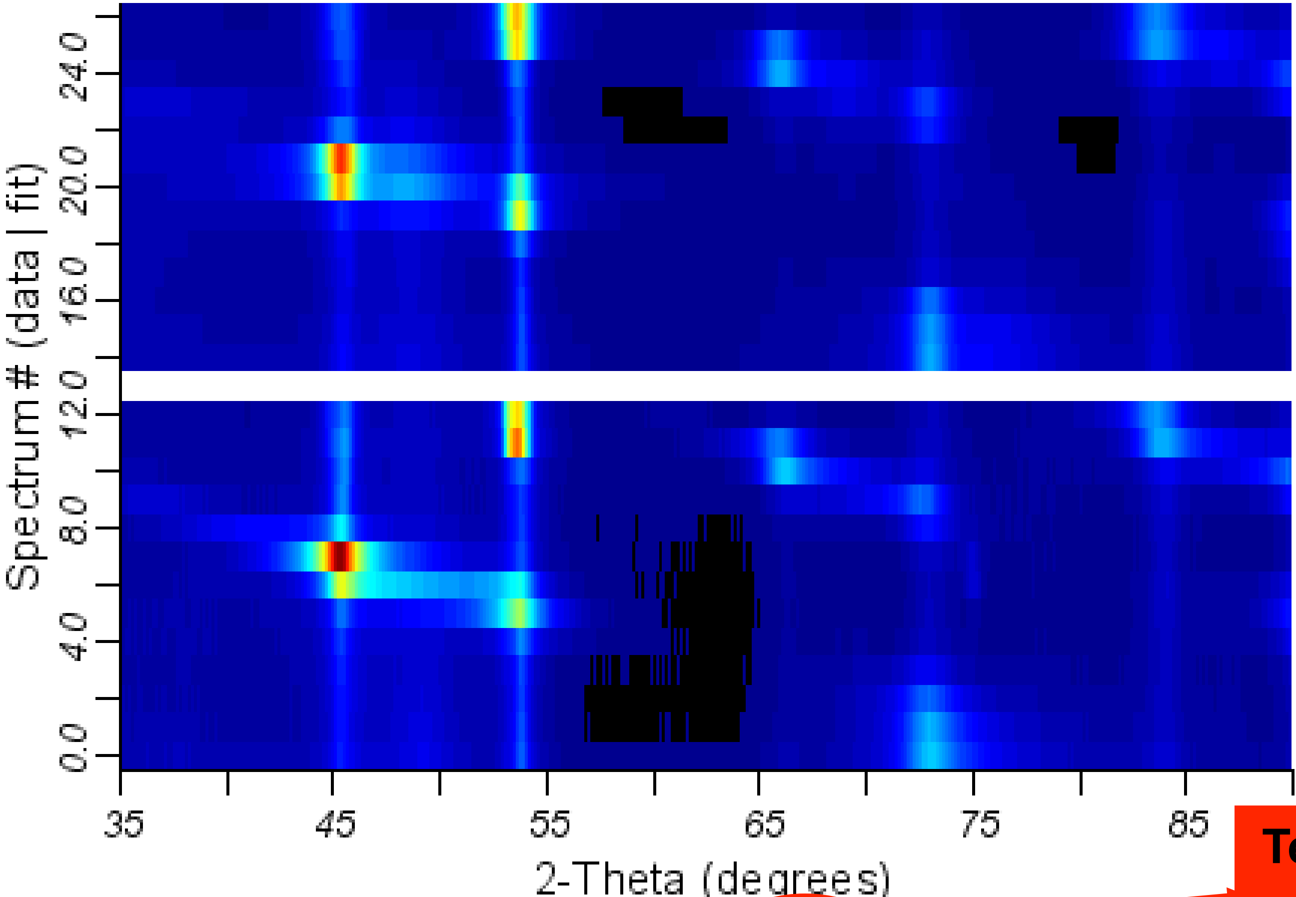

Fibre strong textures + 2 phases + anisotropic crystallite shape + residual strains!

R_{exp} = 11.1%
R_W = 25.7%

% H-ZnSe = 45.4%

Tensile in plane stress ≠ Rizzo et al.

Phase	Cell parameters (Å)	In-plane stress (MPa)	Anisotropic sizes (Å)			
			[111]	[100]	[110]	[103]
C-ZnSe	a = 5.6497(3)	263 (14)	112 (1)	117 (5)	85(1)	-
H-ZnSe	a= 3.9527(6) c = 6.7154(8)	436 (25)	-	244 (1)	244 (2)	20(2)

Multiphased Cr^{2+}:ZnSe films : combined analysis approach actual imitations

C-ZnSe texture :

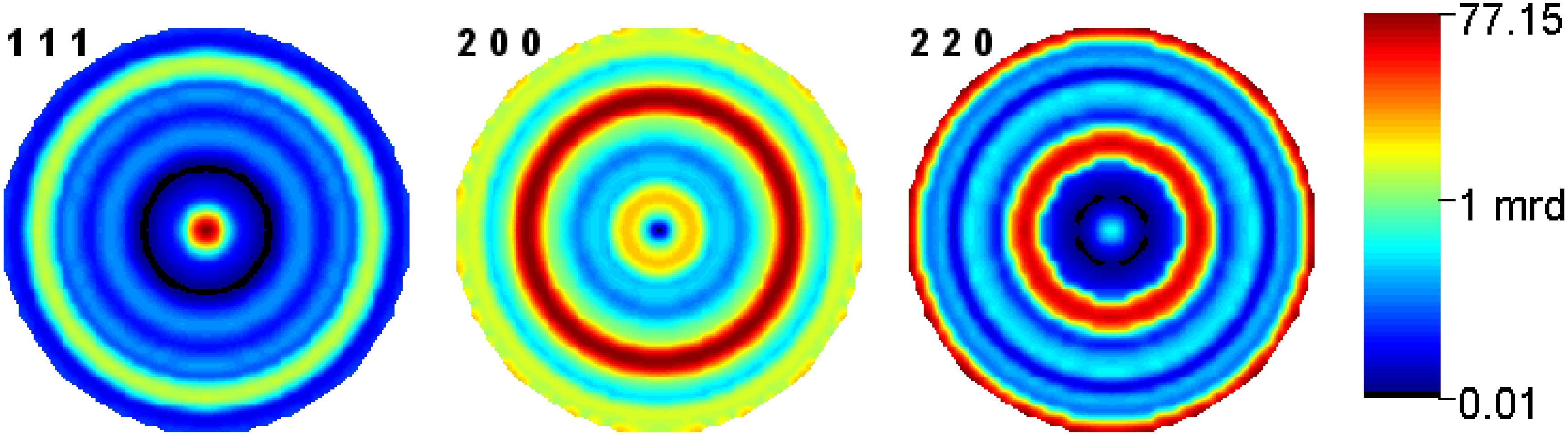

strong <111> fibre texture with some residual orientations

H-ZnSe texture :

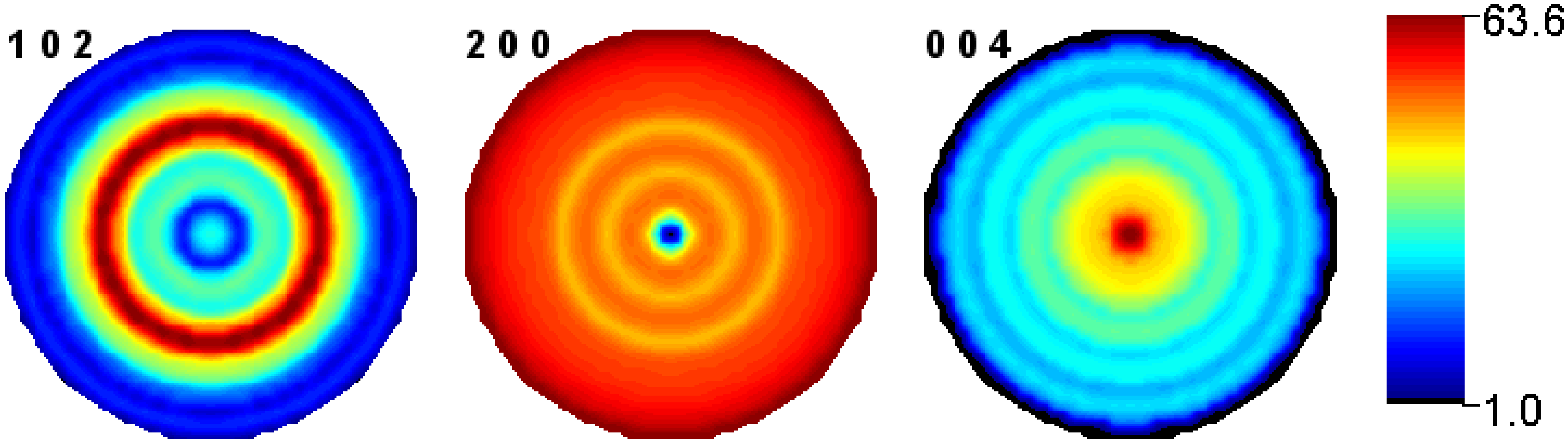

unique <001> strong fibre texture

Refined fibre like textures independent of the substrate choice !

HRTEM image

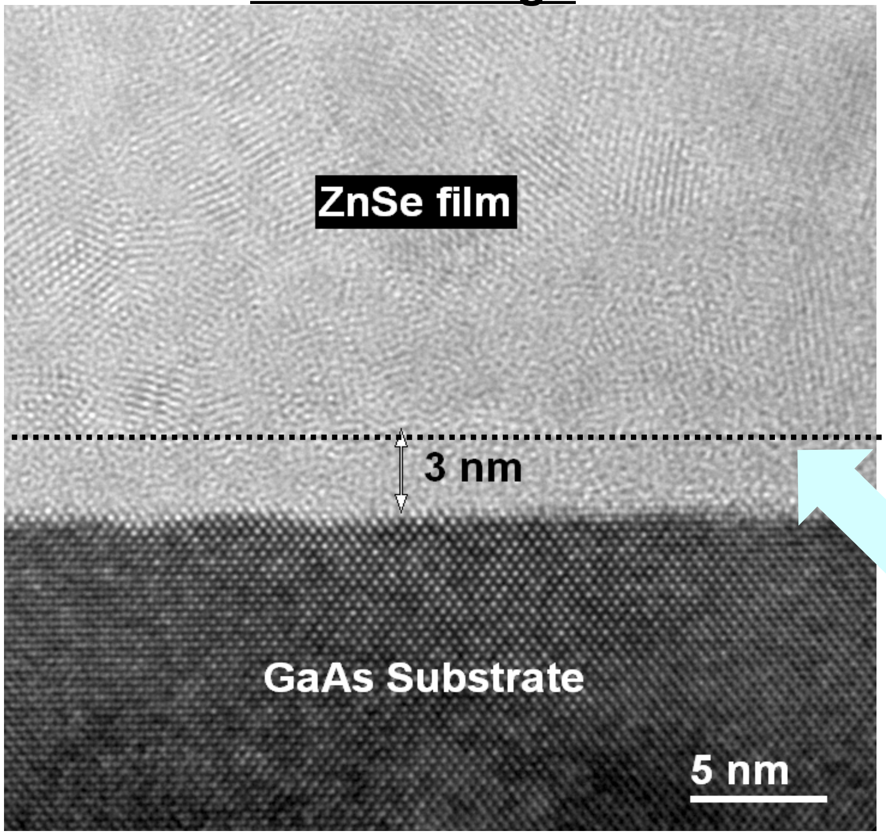

Bright field TEM image

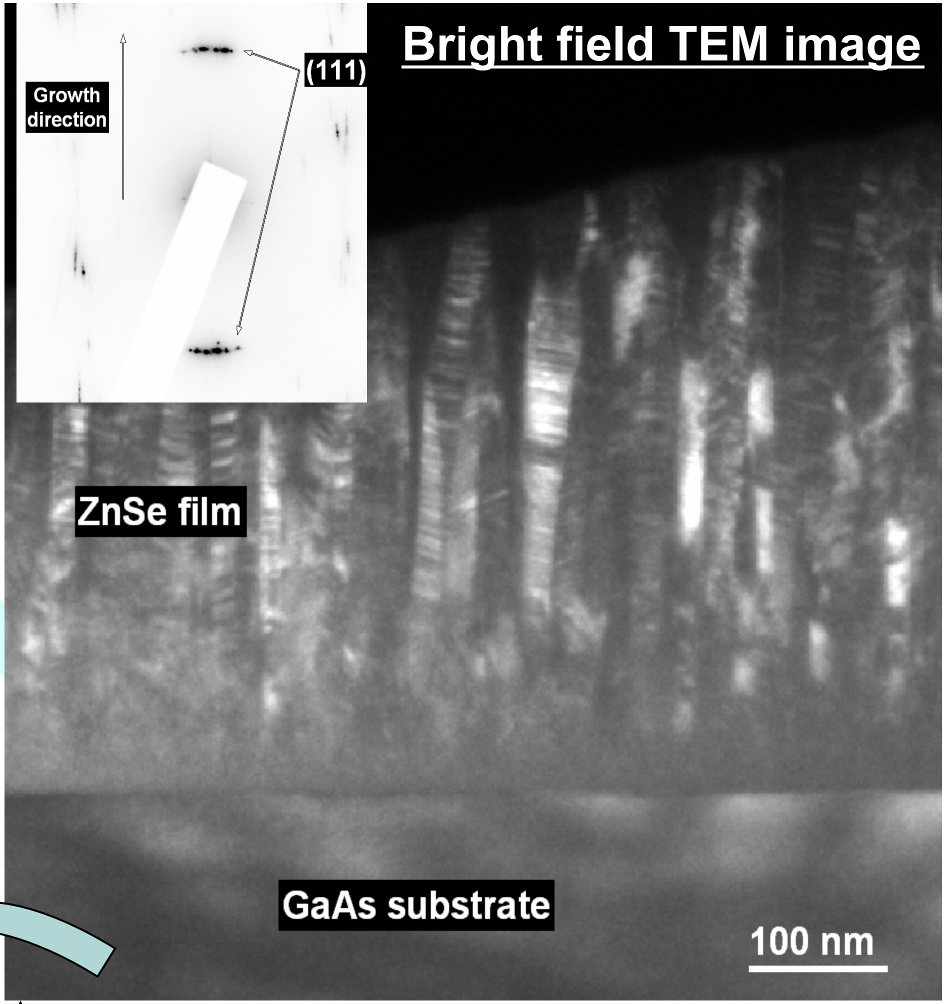

Strong <111> texture for the C-ZnSe
+ twin faults evidenced in H-ZnSe

χ −sum diagram at ω =13.65° with residual strains: fit still not optimum!!

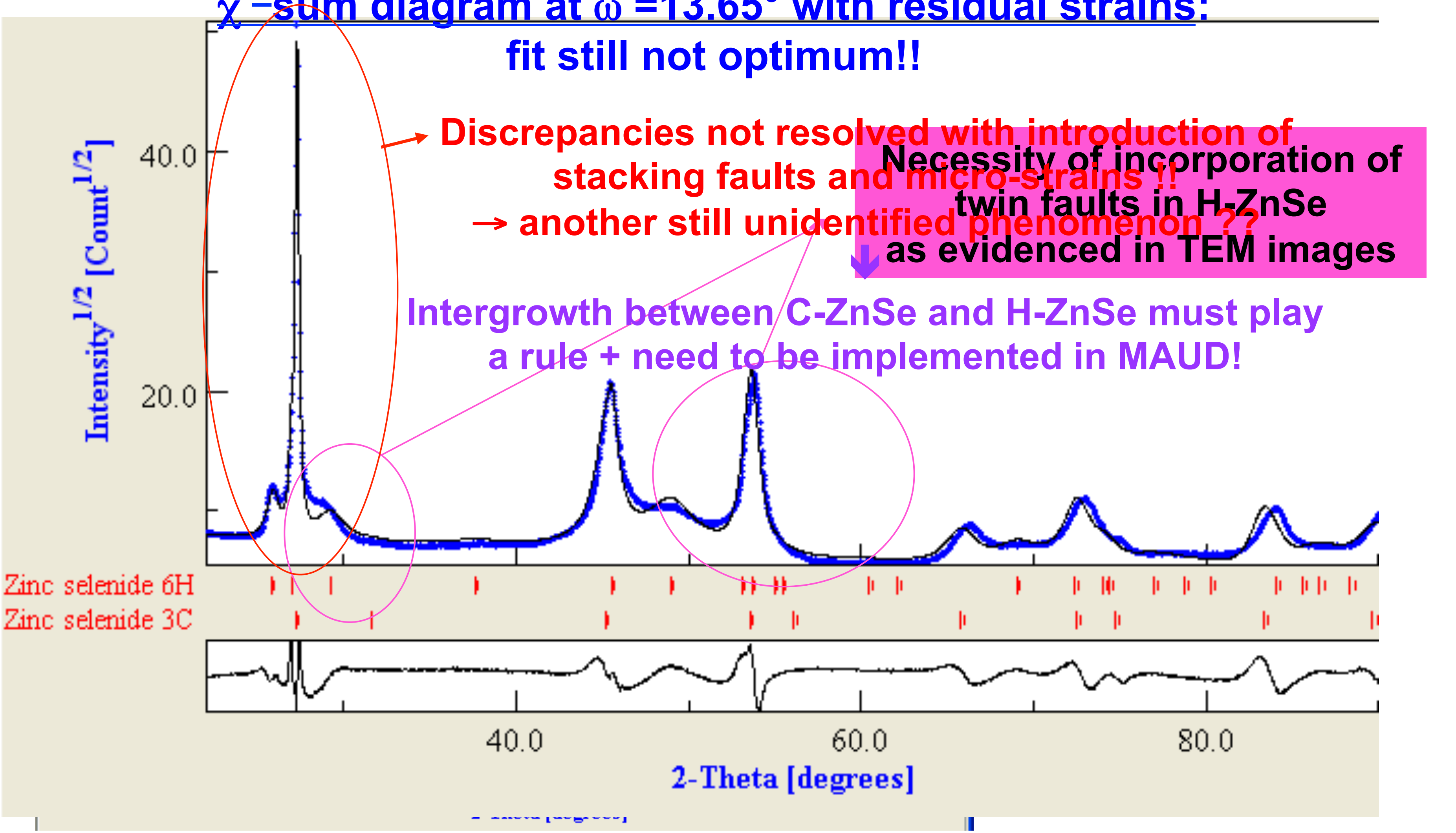

Better reproduction for 2θ > 35° with H-ZnSe twin faults probability of 45.7 (6)%;
but still discrepancies for 2θ < 35° !!!

THANK YOU FOR YOUR ATTENTION !!!